October 11, 1999

# TOTAL IONIZATION DOSE TEST REPORT

*No. 99T-RT14100-72*
*J. J. Wang*
*(408)522-4576*
*jih-jong.wang@actel.com*

## 1.0 SUMMARY TABLE

| A14100A Parametrics/Characteristics | Results |
|---|---|
| 1. Functionality | Not tested to the limit, Passed 20krad(Si) |
| 2. $I_{DDSTDBY}$ | Passed 20krad(Si) (Figure) |
| 3. $V_{IL}/V_{IH}$ | Passed 20krad(Si) |
| 4. $V_{OL}/V_{OH}$ | Passed 20krad(Si) |
| 5. Propagation Delays | Passed 20krad(Si) |
| 6. Rising/Falling Edge Transient | Passed 20krad(Si) |
| 7. Startup Transient Current | Passed 20krad(Si) (Figures ) |

## 2.0 TID TEST

This section describes the device under test (DUT), the irradiation parameters, and the testing method.

### 2.1 TEST DEVICE

Table 1 lists the DUT information.

Table 1. DUT Information

| | |
|---|---|
| Part Number | RT14100A |
| Package | CQFP256 |
| Foundry | MEC |
| Technology | 0.8µm CMOS |
| Die Lot Number | UCL072 |
| Quantity Tested | 5 |
| Serial Numbers | LAN905 (control), LAN2001, LAN2002, LAN2003, LAN2004 |

### 2.2 IRRADIATION

Table 2 lists the irradiation parameters.

Table 2. Irradiation Parameters

| | |
|---|---|
| Facility | NASA |
| Radiation Source | Co-60 |
| Dose Rate | 6krad(Si)/day (+-10%) |
| Final Total Dose | 20krad(Si) |
| Temperature | Room |
| Bias | 5V |

## 2.3 TEST METHOD

The test method is in compliance with TM1019. It uses the biased room-temperature anneal to simulate the extremely slow-dose-rate space environment. Figure 1 shows the process flow. Rebound annealing at 100°C is omitted because there are enough data showing antifuse FPGAs fabricated in MEC foundry have no rebound effects (see, for example, the recent TID Report No. 98-T14100-2).

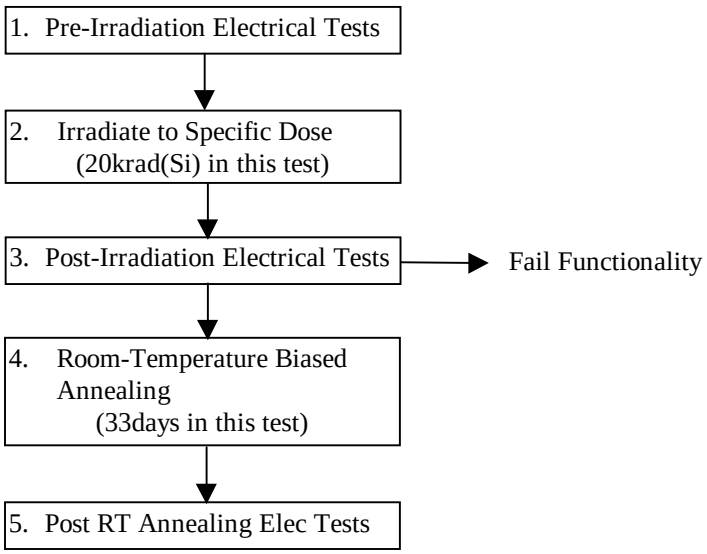


Figure 1. Test method flow chart.

## 2.4 ELECTRICAL PARAMETERS/CHARACTERISTICS TESTS

The electrical parameters/characteristics were measured on the bench. Compared to an automatic tester, this bench setup has much lower noise. For AC/DC characteristics measurement, the automatic tester can measure every possible pin while the bench setup only samples few pins (due to logistics, not inability). However, since the total dose tolerance is always limited by the $I_{DDstandby}$, not by AC/DC characteristics, sampling pins for AC/DC characteristics should be enough. Also, $I_{DDstandby}$ is best measured by a bench setup. For example, the in-situ monitoring during irradiation done in this report is logistically impossible for an automatic tester. An important but non-standard parameter, startup transient current, basically can only be measured on the bench too. The corresponding logic design circuit for each test parameter is listed in Table 3.

Table 3. Logic Design for each Measured Parameter/Characteristic

| Parameter/Characteristics | Logic Design |
|---|---|
| 1. Functionality | All key architectural functions |
| 2. $I_{DDSTDBY}$ | DUT power supply |
| 3. $V_{IL}/V_{IH}$ | TTL compatible input buffer |
| 4. $V_{OL}/V_{OH}$ | TTL compatible output buffer |
| 5. Propagation Delays | String of inverters |
| 6. Rising/Falling Edge | D flip-flop output |

| | |
|---|---|
| 7. Startup Transient Current | DUT power supply |

## 3.0 TEST RESULTS

This section presents all the parameter/characteristic results for pre-irradiation (step 1 in Figure 1), post-irradiation (step 3), and post room temperature anneal tests (step 5).

### 3.1 FUNCTIONAL TEST

Table 4 lists the functional test results.

Table 4. Functionality Test Results

| | Pre-Irradiation | Post-Irradiation | Post-Anneal |
|---|---|---|---|
| LAN905 (cntl) | passed | passed | passed |
| LAN2001 | passed | passed | passed |
| LAN2002 | passed | passed | passed |
| LAN2003 | passed | passed | passed |
| LAN2004 | passed | passed | passed |

### 3.2 IDDSTANDBY

$I_{DDstandby}$ (labeled $I_{CC}$ in some Figures) was monitored during the irradiation and room-temperature anneal. The delta $I_{DDstandby}$ is the increment $I_{DDstandby}$ due to irradiation/anneal effect. Compared to the spec of 25mA, the small (< 1mA) pre-irradiation $I_{DDstandby}$ is negligible. Thus the delta $I_{DDstandby}$ spec is approximately 25mA.

As shown in Figure 2, four DUTs, LAN2001, LAN2002, LAN2003 and LAN2004 were irradiation to just over 20krad(Si). The worst case is LAN2003, with final $I_{DDstandby}$ ~ 29mA. Since all DUTs passed post-irradiation functional test, per TM1019, room temperature, $V_{CC}$ (5V) biased annealing can be performed to reduce the leakage current ($I_{DDstandby}$). Figure 2 shows the reduction of leakage with respect to annealing time. After 33 days anneal, all DUTs have $I_{DDstandby}$ no more than 3mA.

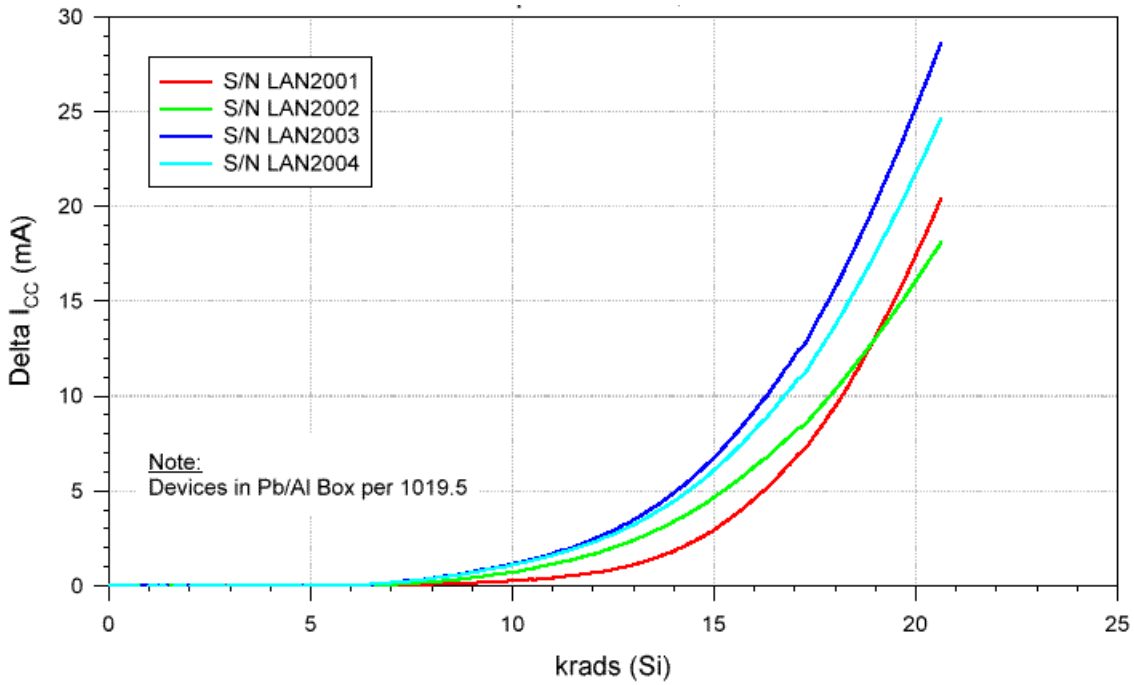


Figure 2. Delta $I_{DDstandby}$ versus total cumulative dose.

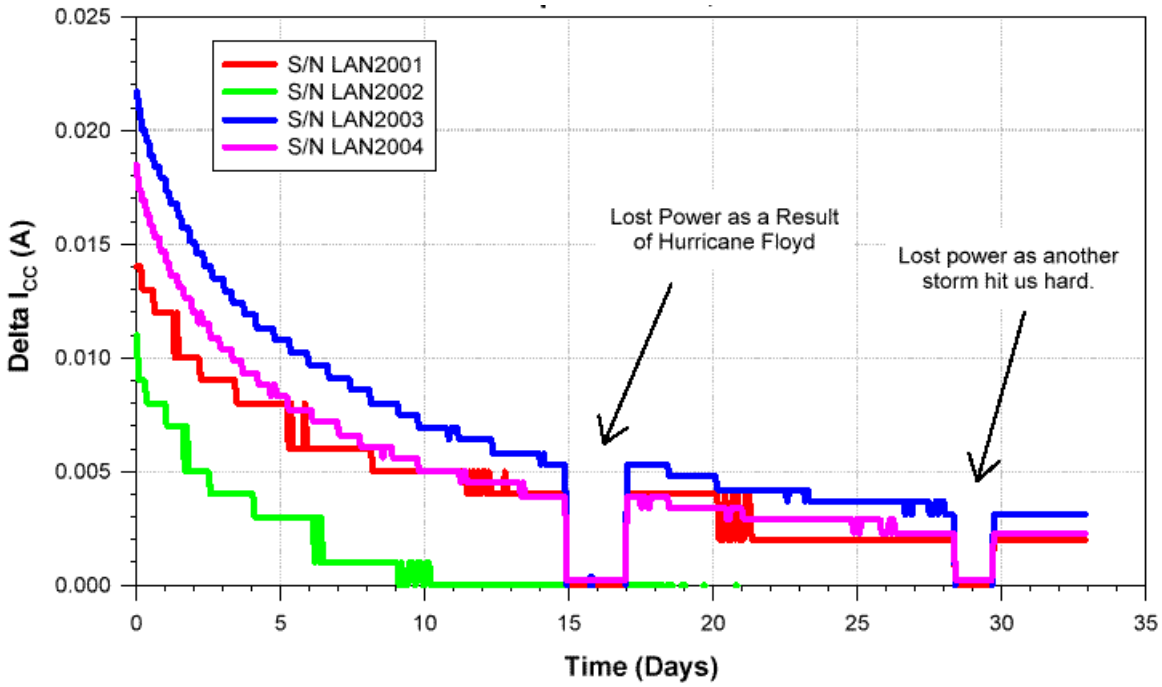


Figure 3. Showing the reduction of $I_{DDstanby}$ by room temperature annealing.

### 3.3 INPUT LOGIC THRESHOLD

Table 5 lists the input logic threshold of each DUT for pre-irradiation, post-irradiation and post room-temperature anneal test.

Table 5. Input Logic Threshold ($V_{IL}/V_{IH}$) Results

| | Pre-Irradiation | Post-Irradiation | Post-Anneal |
|---|---|---|---|
| LAN905 (cntl) | 1.19V | 1.19V | 1.25V |
| LAN2001 | 1.19V | 1.21V | 1.29V |
| LAN2002 | 1.19V | 1.20V | 1.27V |
| LAN2003 | 1.19V | 1.21V | 1.28V |
| LAN2004 | 1.17V | 1.20V | 1.27V |

### 3.4 OUTPUT CHARACTERISTIC

Figure 4a and 4b show the $V_{OL}$ characteristic curve for pre-irradiation and post-irradiation respectively. For each DUT, both pre- and post-irradiation test passed the spec, and no significant radiation effect can be identified. For the reference, the spec is, at $I_{OL}$ = 6mA, $V_{OL}$ cannot exceed 0.4V.

Figure 5a and 5b show the $V_{OH}$ characteristic curve for pre-irradiation and post-irradiation respectively. For each DUT, both pre- and post-irradiation test passed the spec, and the radiation effect is negligible. The spec is, at $I_{OH}$ = 4mA, $V_{OH}$ cannot be lower than 3.7V.

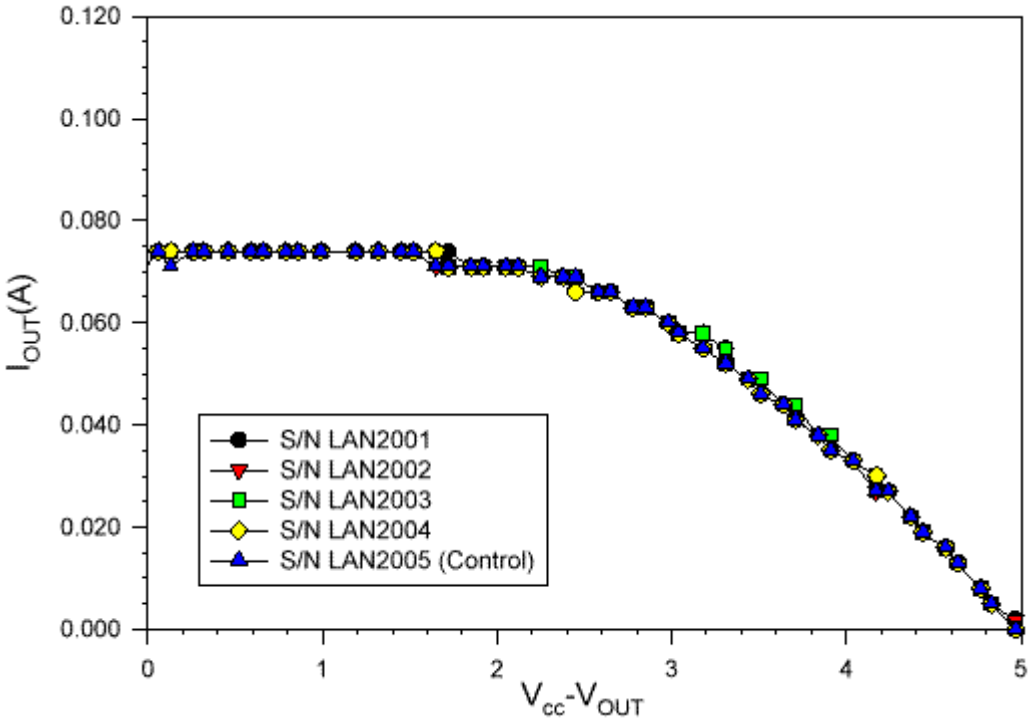


Figure 4a. Pre-irradiation $V_{OL}$ characteristic curve.

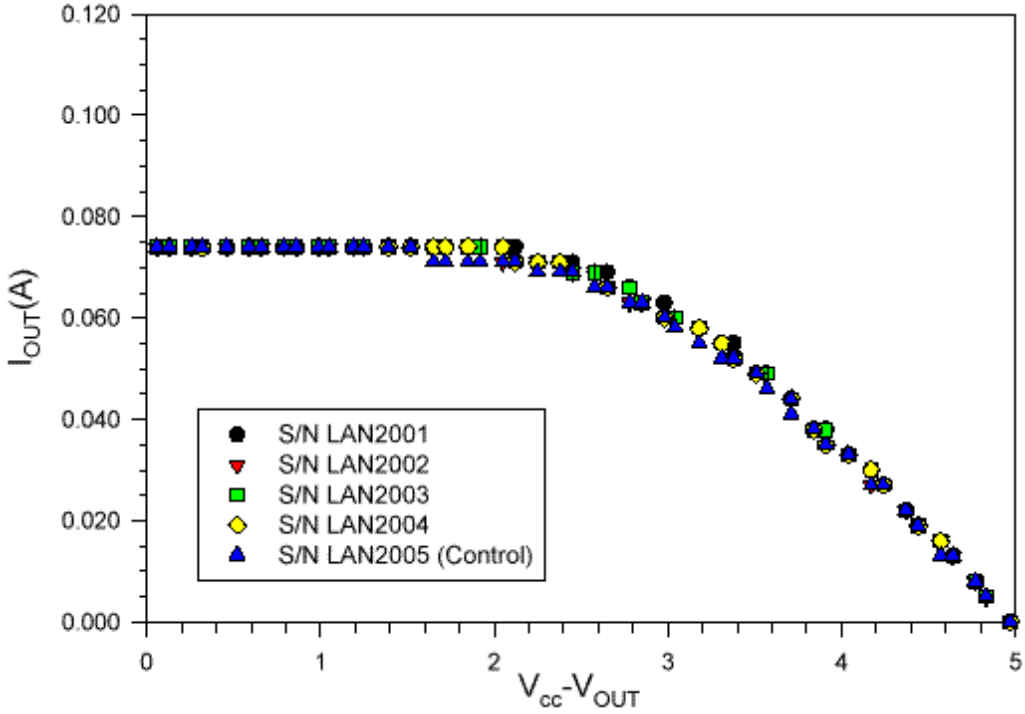


Figure 4b. Post-irradiation $V_{OL}$ characteristic curve.

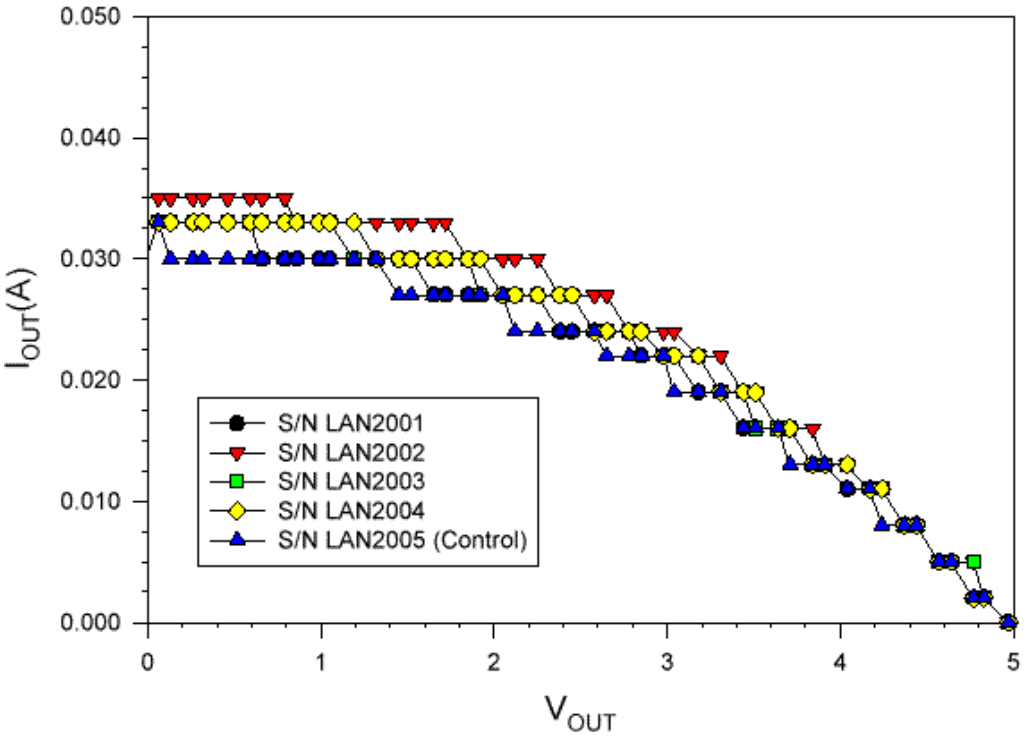


Figure 5a. Pre-irradiation $V_{OH}$ characteristic curve

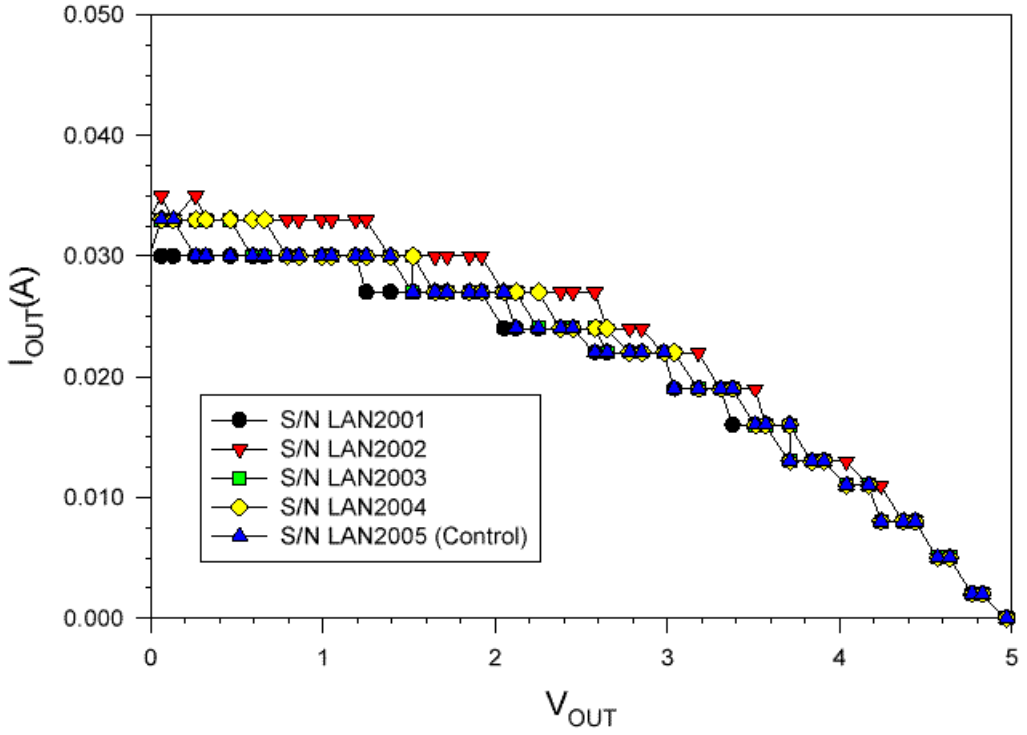


Figure 5b. Post-irradiation $V_{OH}$ characteristic curve

## 3.5 PROPAGATION DELAYS

Three types of propagation delays were measured, a combinational logic, the clock to Q delay of a serial-in shift register, and the clock to Q of a serial-out shift register. The rising edge and falling edge were measured separately. The following Table 6, 7 and 8 list the results. The variation due to irradiation/annealing effect is always well within 10%.

Table 6. Propagation Delay of Combinational Logic (ns)

| | Rising Output | | | Falling Output | | |
|---|---|---|---|---|---|---|
| | Pre-Irradiation | Post-Irradiation | Post-Anneal | Pre-Irradiation | Post-Irradiation | Post-Anneal |
| LAN905(cntl) | 934 | 926 | 932 | 933 | 925 | 931 |
| LAN2001 | 938 | 967 | 950 | 937 | 953 | 939 |
| LAN2002 | 899 | 899 | 905 | 897 | 886 | 895 |
| LAN2003 | 920 | 933 | 930 | 919 | 920 | 921 |
| LAN2004 | 914 | 926 | 928 | 913 | 914 | 918 |

Table 7. Clock to Q Delay of Serial-In Shift Register (ns)

| | Rising Output | | | Falling Output | | |
|---|---|---|---|---|---|---|
| | Pre-Irradiation | Post-Irradiation | Post-Anneal | Pre-Irradiation | Post-Irradiation | Post-Anneal |
| LAN905(cntl) | 9.5 | 9.5 | 9.8 | 9.6 | 9.4 | 9.8 |
| LAN2001 | 9.6 | 9.6 | 10.1 | 9.7 | 9.8 | 10.3 |
| LAN2002 | 10.2 | 9.3 | 9.7 | 9.8 | 9.7 | 9.9 |
| LAN2003 | 10.4 | 9.9 | 10.0 | 10.4 | 10.1 | 10.2 |
| LAN2004 | 10.2 | 9.8 | 9.8 | 10.3 | 9.9 | 10.1 |

Table 8. Clock to Q Delay of Serial Out Shift Register (ns)

| | Rising Output | | | Falling Output | | |
|---|---|---|---|---|---|---|
| | Pre-Irradiation | Post-Irradiation | Post-Anneal | Pre-Irradiation | Post-Irradiation | Post-Anneal |
| LAN905(cntl) | 5.7 | 6.2 | 6.4 | 5.4 | 5.4 | 5.8 |
| LAN2001 | 6.0 | 6.2 | 6.5 | 5.5 | 5.7 | 5.8 |
| LAN2002 | 6.3 | 5.3 | 6.1 | 5.9 | 5.0 | 5.5 |
| LAN2003 | 6.5 | 6.3 | 6.4 | 5.9 | 5.6 | 5.8 |
| LAN2004 | 6.7 | 6.0 | 6.3 | 6.1 | 5.3 | 5.7 |

## 3.6 RISING/FALLING EDGE TRANSIENT

The rising and falling edge transient of the output of a D flip-flop in the DUT were measured pre-irradiation, post-irradiation, and post-anneal. Figures 6-10 show the rising edge transient. Figures 11-15 show the falling edge transient. The irradiation/annealing effect is basically negligible.

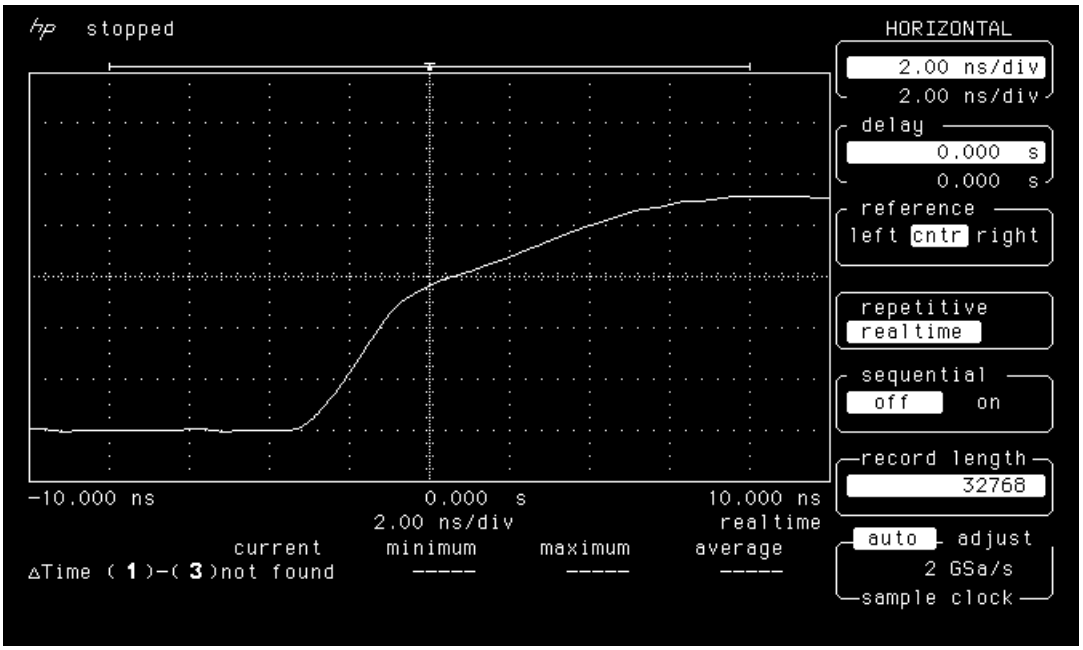


Figure 6a. Rising edge of LAN905 (control) measured with pre-irradiation DUTs.

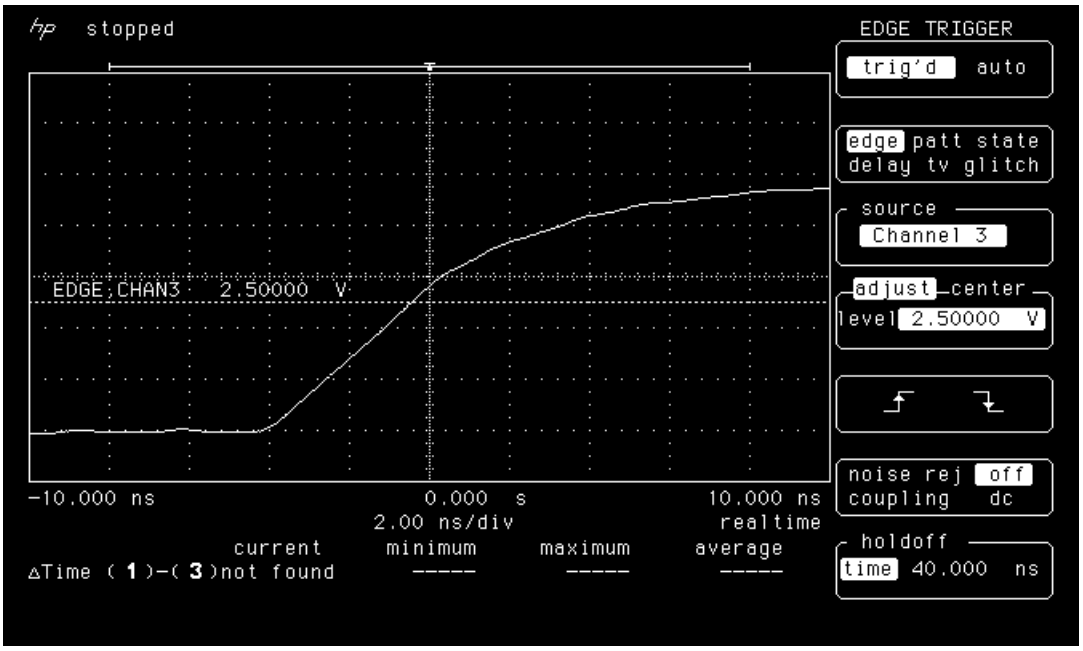


Figure 6b. Rising edge of LAN905 (control) measured with post-irradiation DUTs.

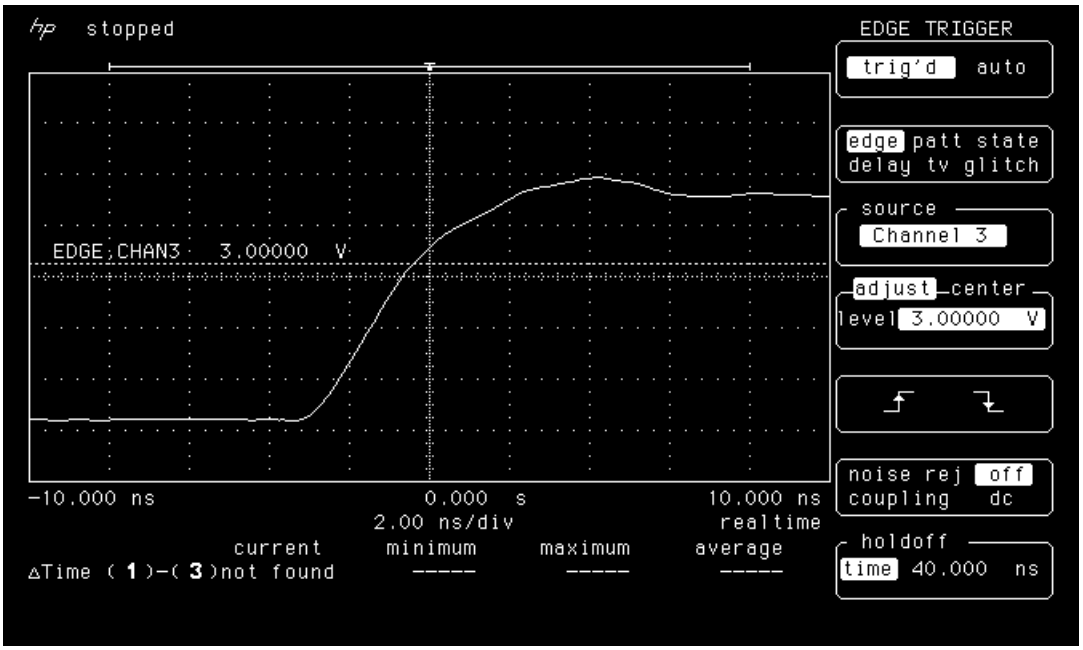


Figure 6c. Rising edge of LAN905 (control) measured with post-anneal DUTs.

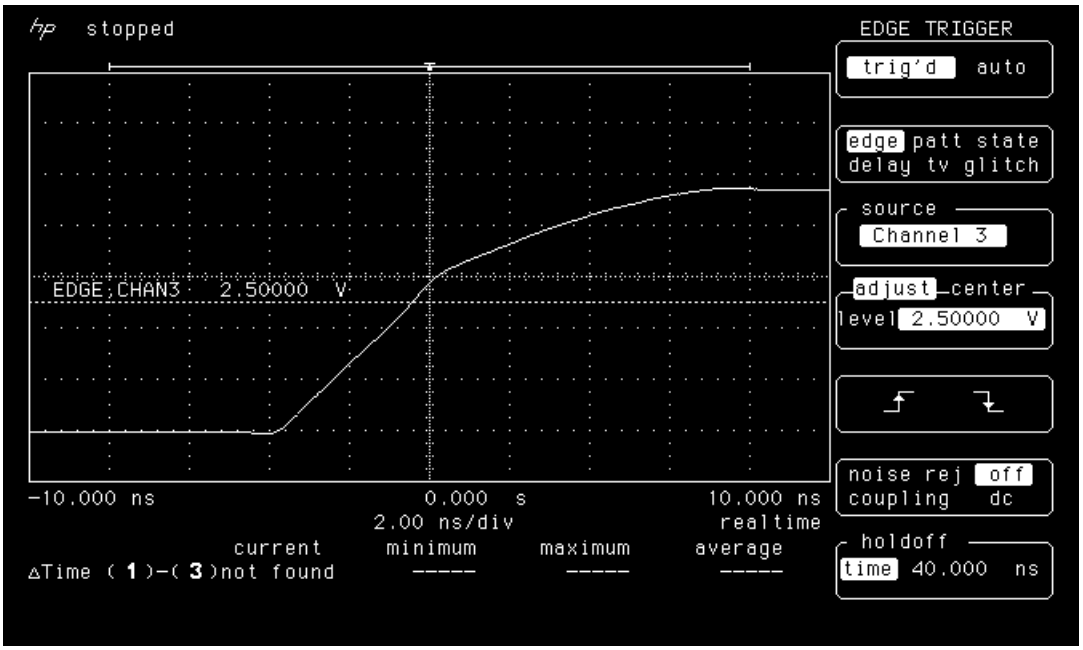


Figure 7a. Rising edge of LAN2001 pre-irradiation.

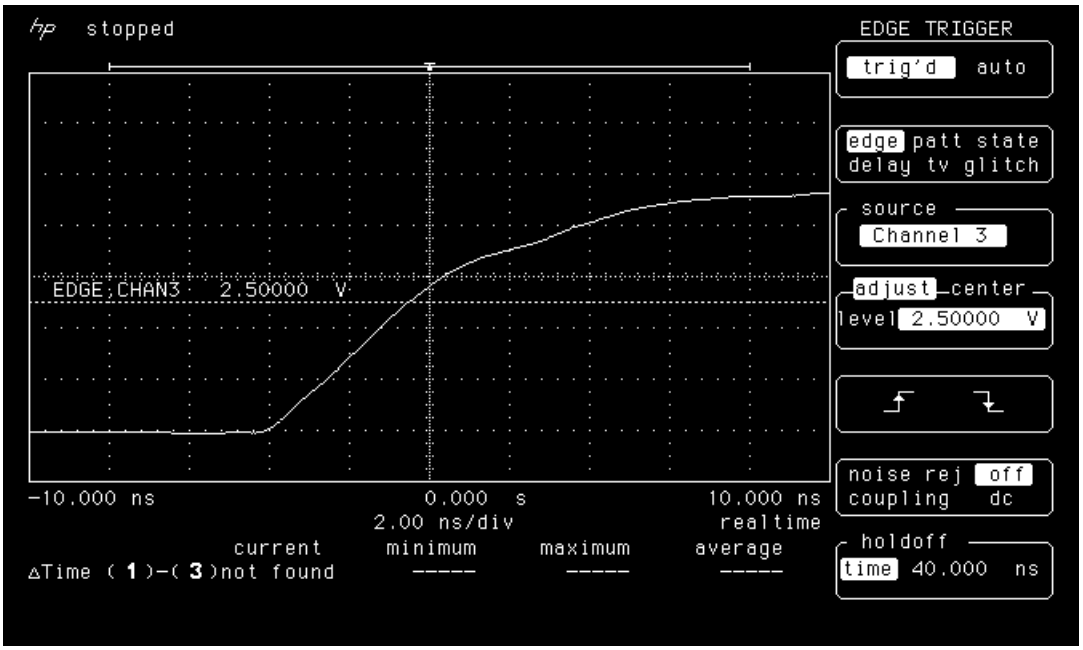


Figure 7b. Rising edge of LAN2001 post-irradiation.

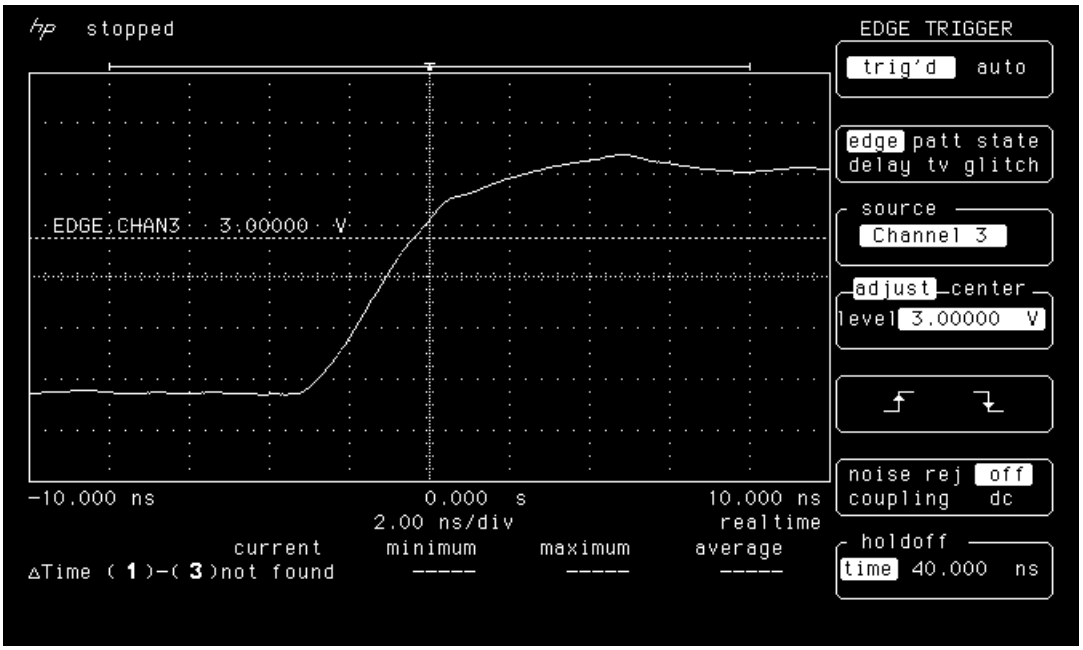


Figure 7c. Rising edge of LAN2001 post-anneal.

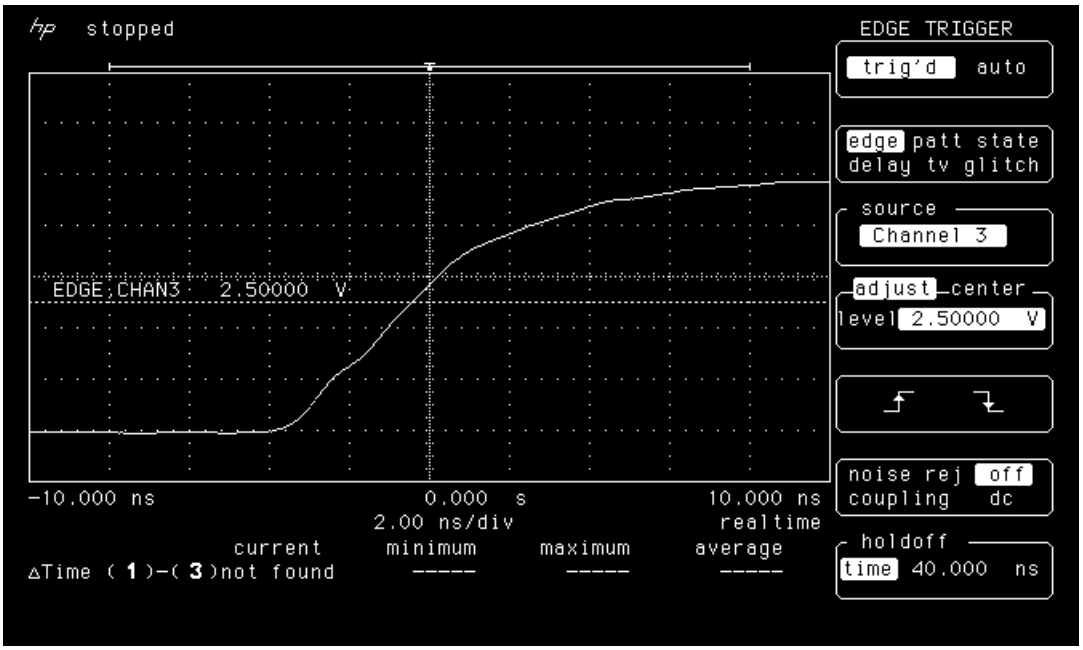


Figure 8a. Rising edge of LAN2002 pre-irradiation.

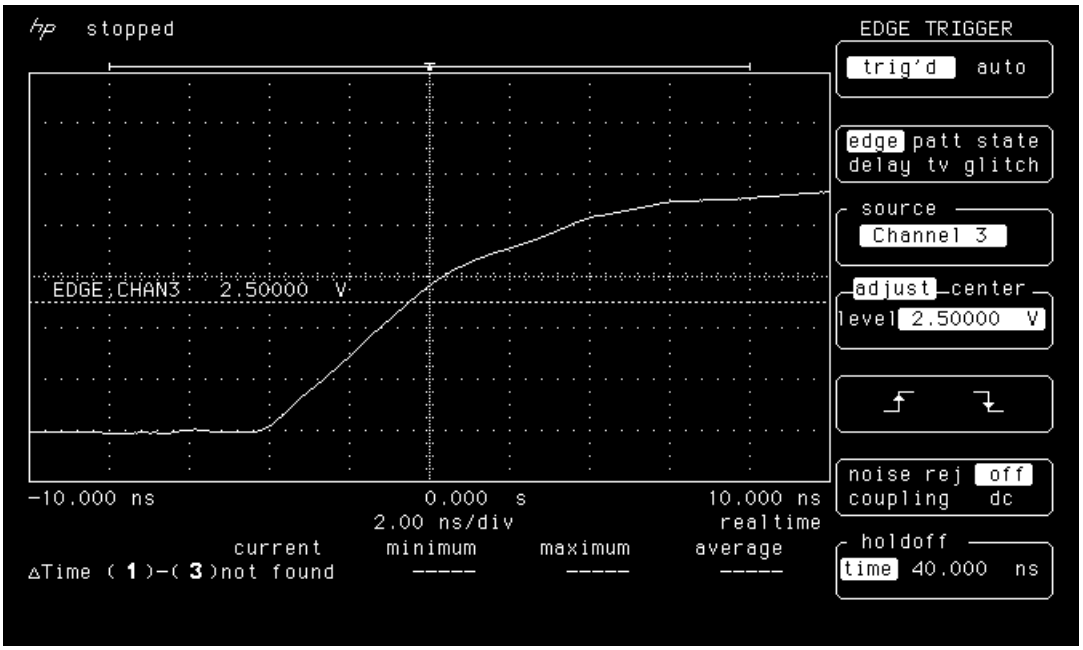


Figure 8b. Rising edge of LAN2002 post-irradiation.

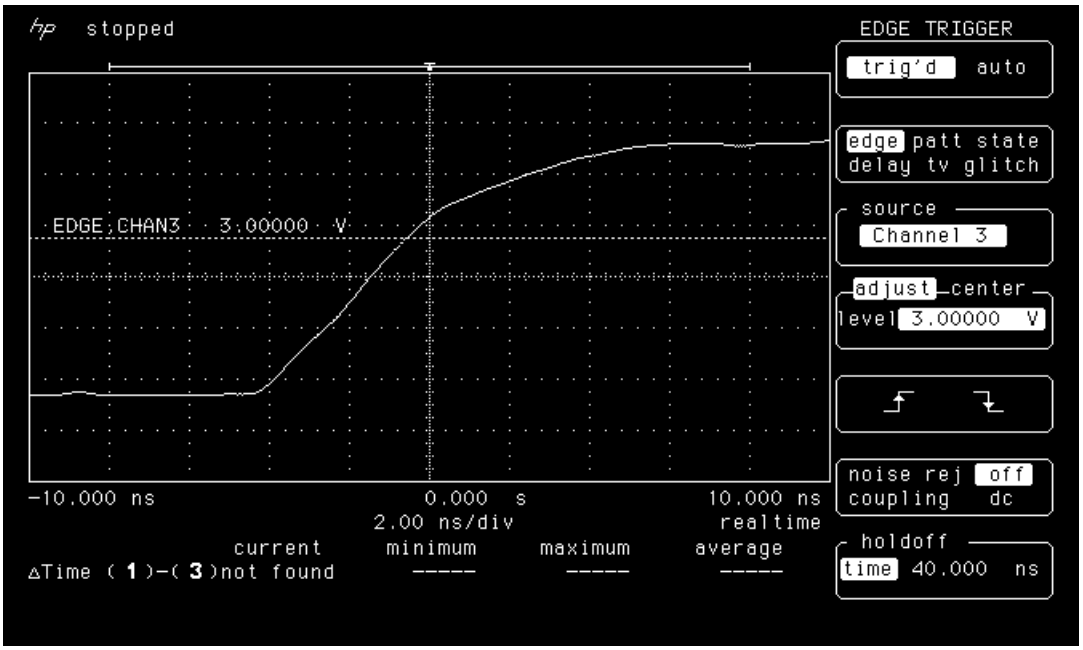


Figure 8c. Rising edge of LAN2002 post-anneal.

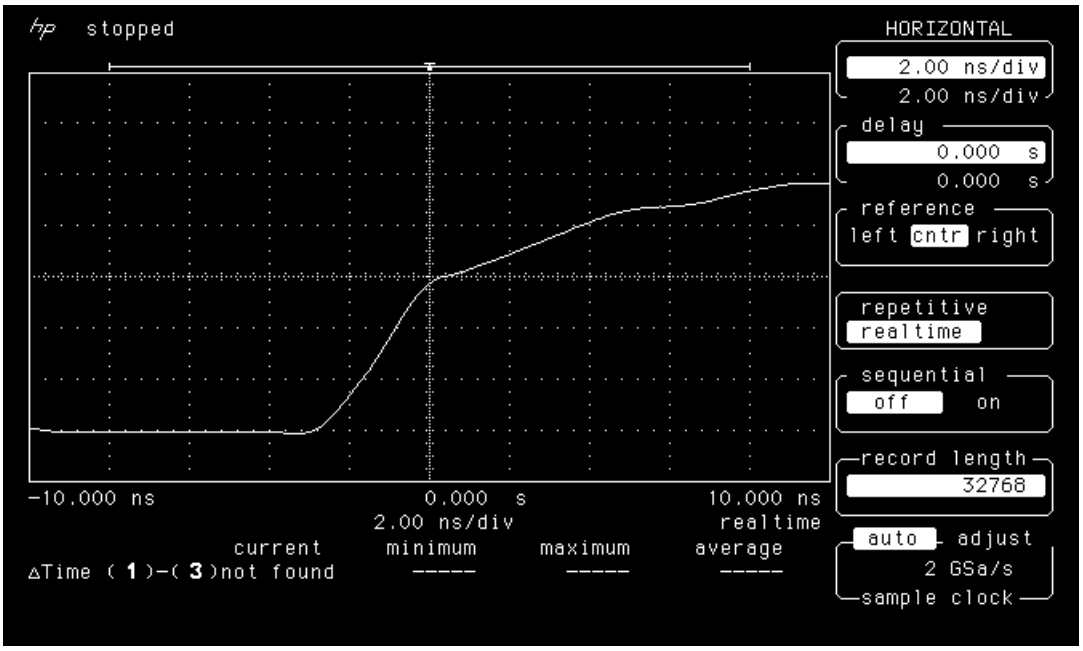


Figure 9a. Rising edge of LAN2003 pre-irradiation

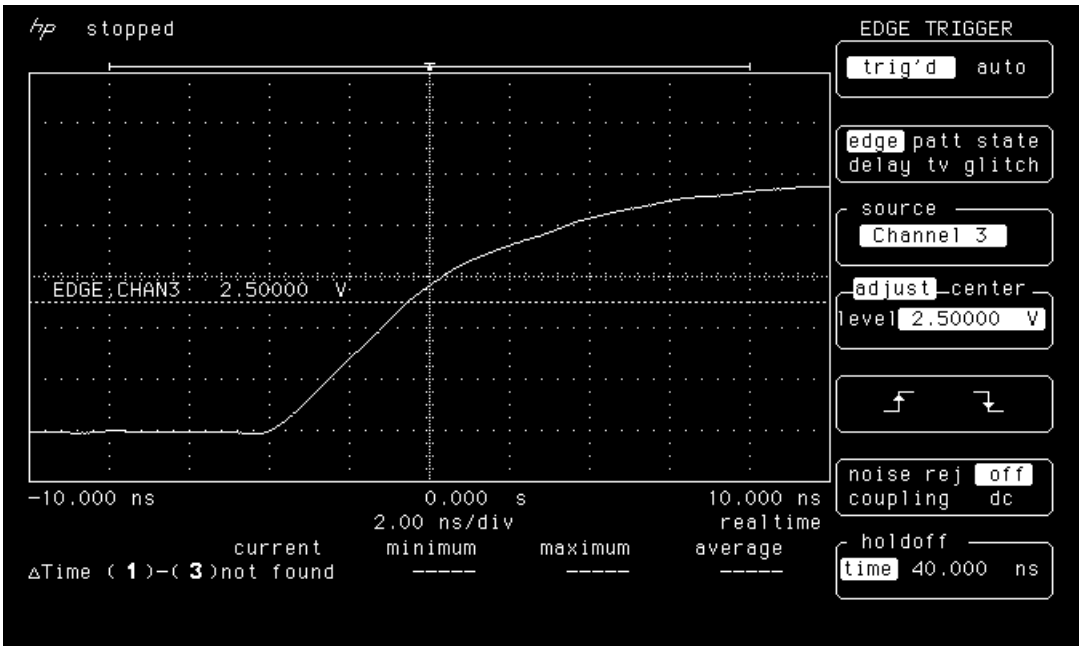


Figure 9b. Rising edge of LAN2003 post-irradiation

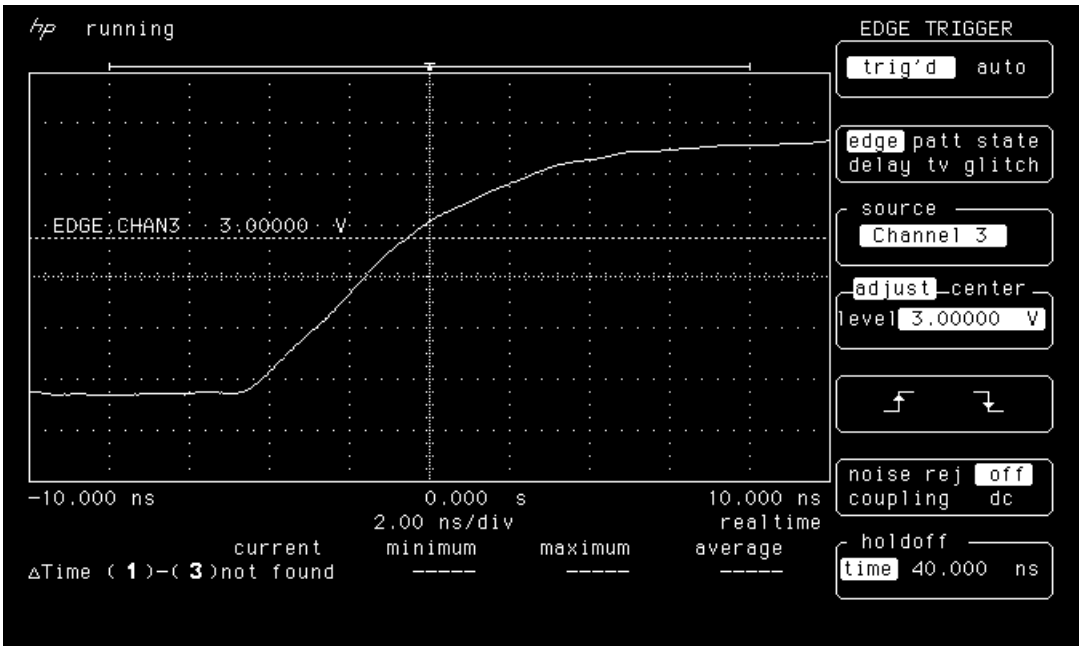


Figure 9c. Rising edge of LAN2003 post-room-anneal.

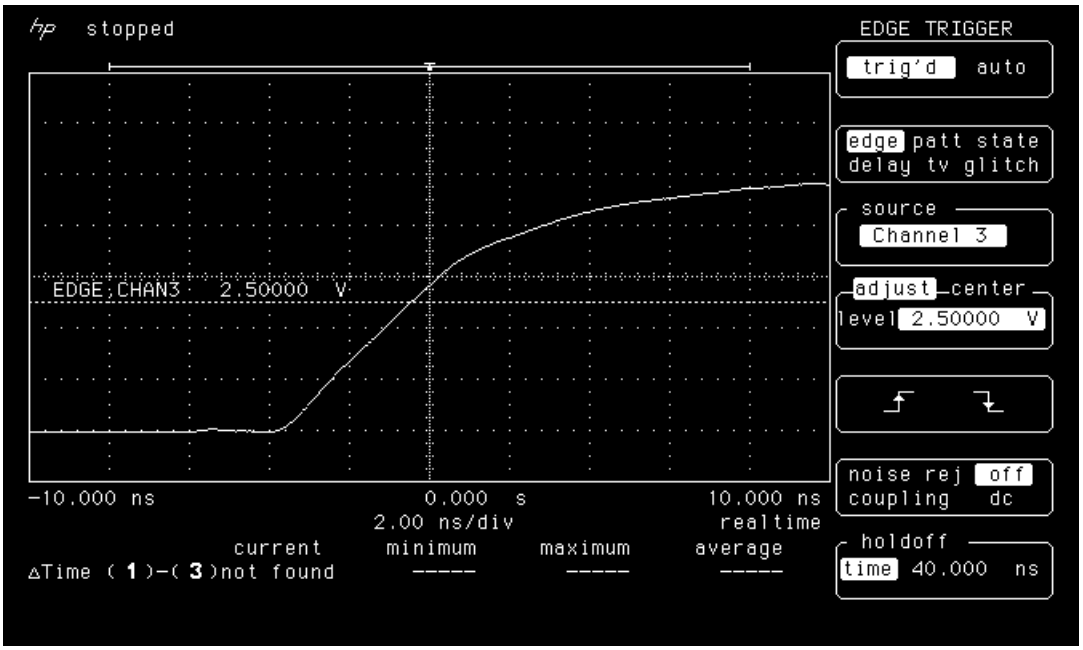


Figure 10a. Rising edge of LAN2004 pre-irradiation.

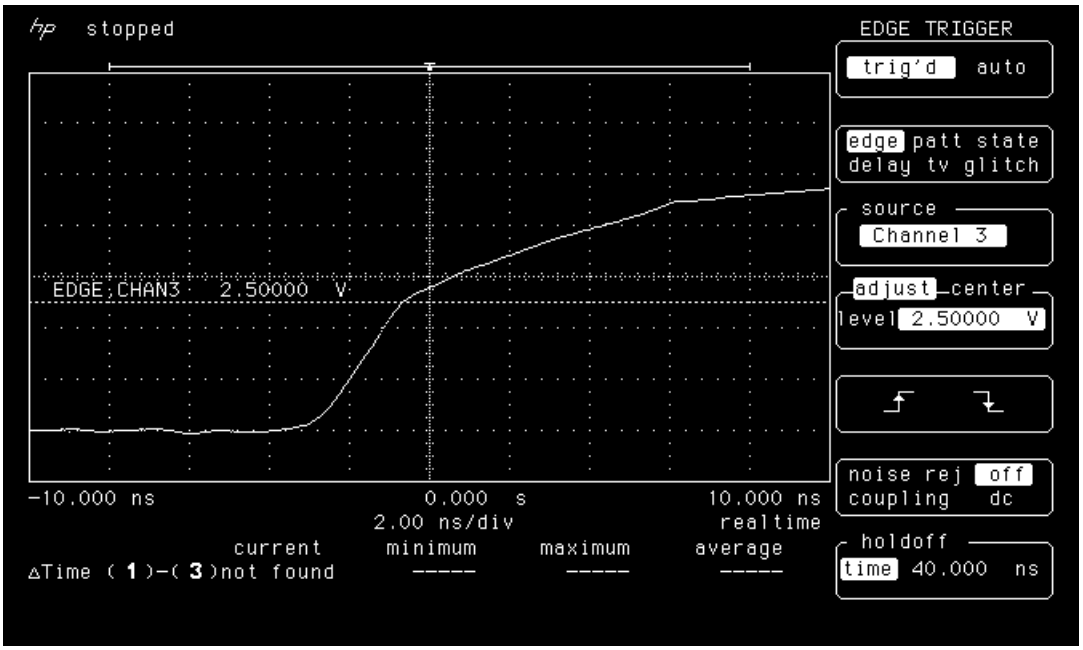


Figure 10b. Rising edge of LAN2004 post-irradiation.

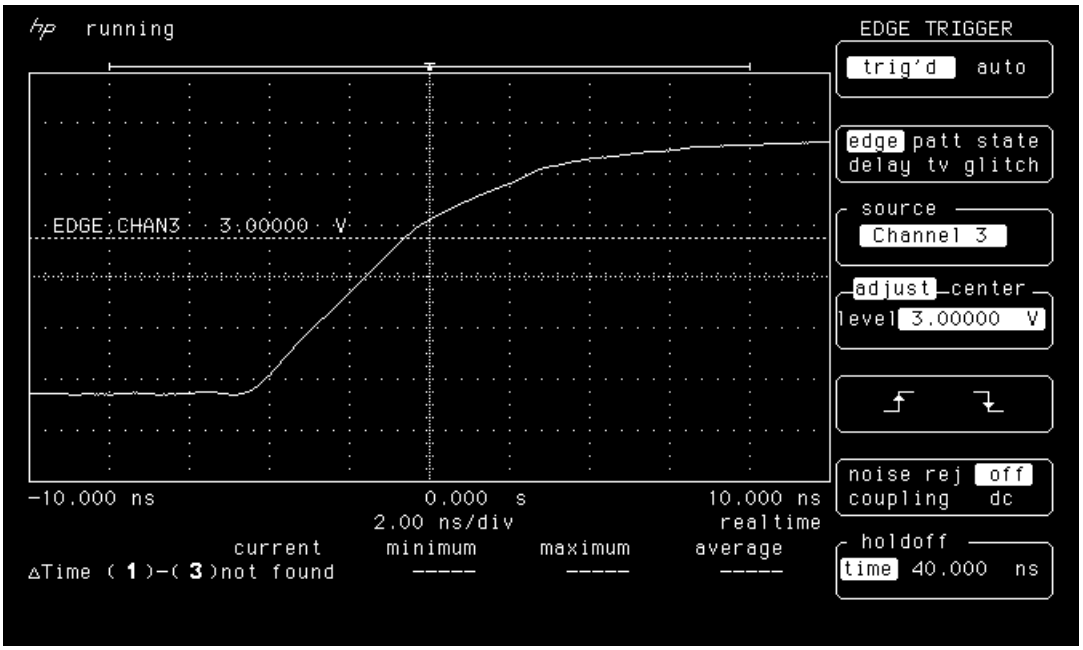


Figure 10c. Rising edge of LAN2004 post-anneal.

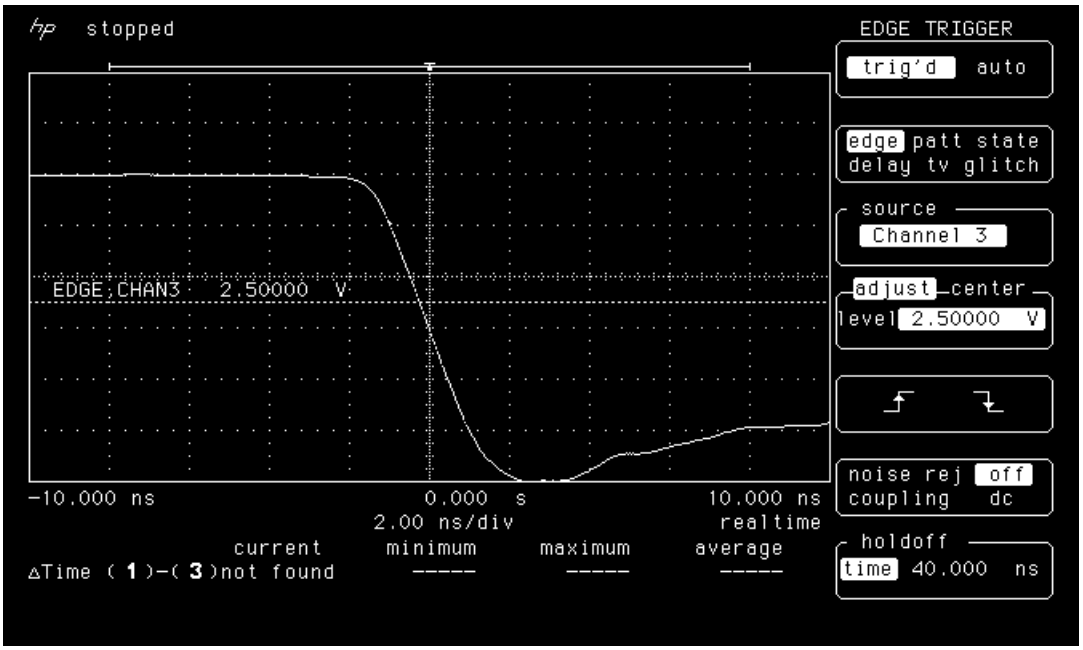


Figure 11a. Falling edge of LAN905 (control) measured with pre-irradiation DUTs.

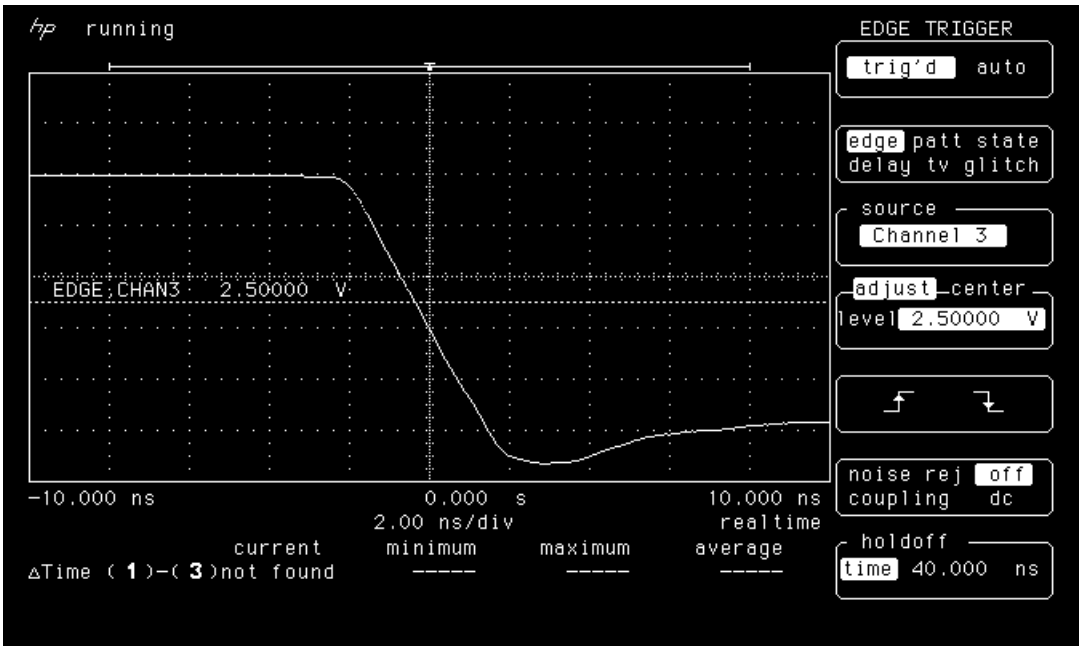


Figure 11b. Falling edge of LAN905 (control) measured with post-irradiation DUTs.

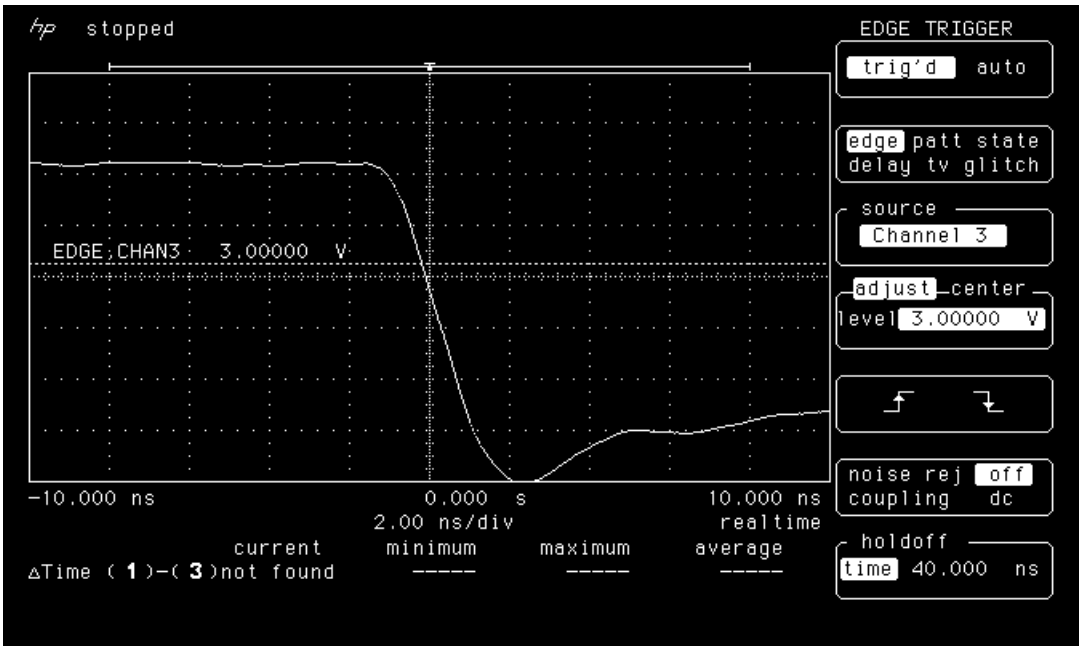


Figure 11c. Falling edge of LAN905 measured with post-anneal DUTs.

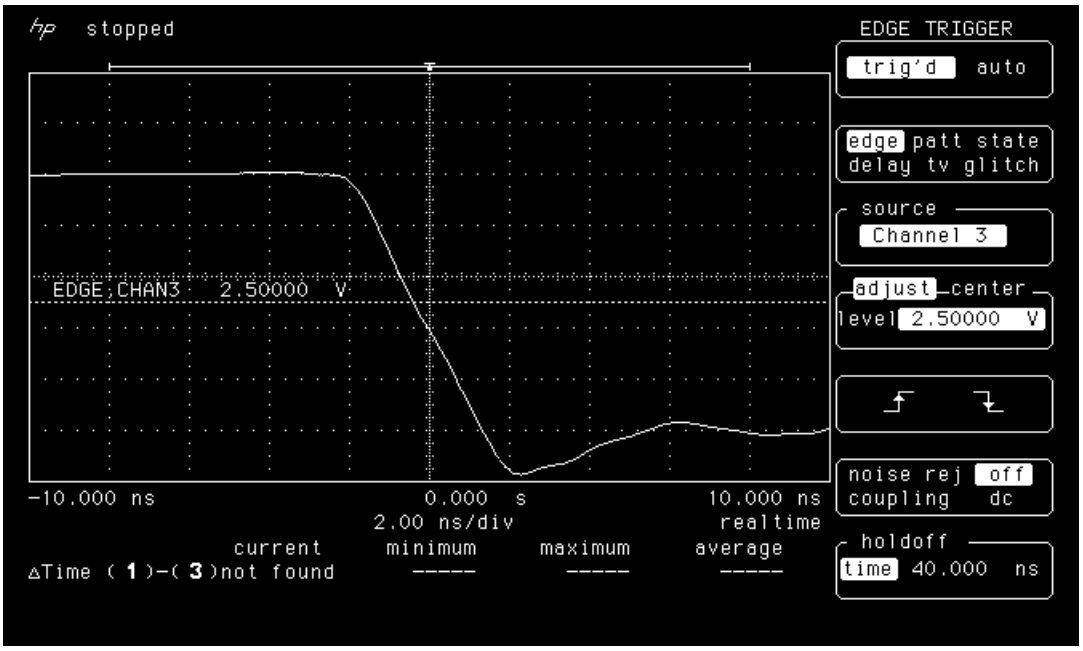


Figure 12a. Falling edge of LAN2001 pre-irradiation.

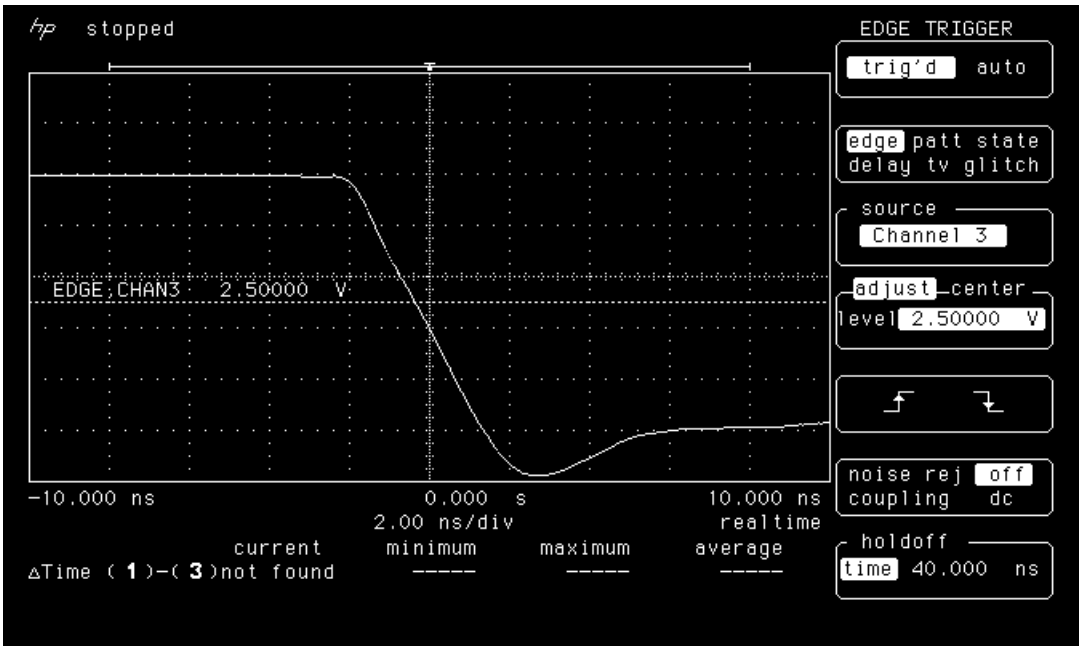


Figure 12b. Falling edge of LAN2001 post-irradiation

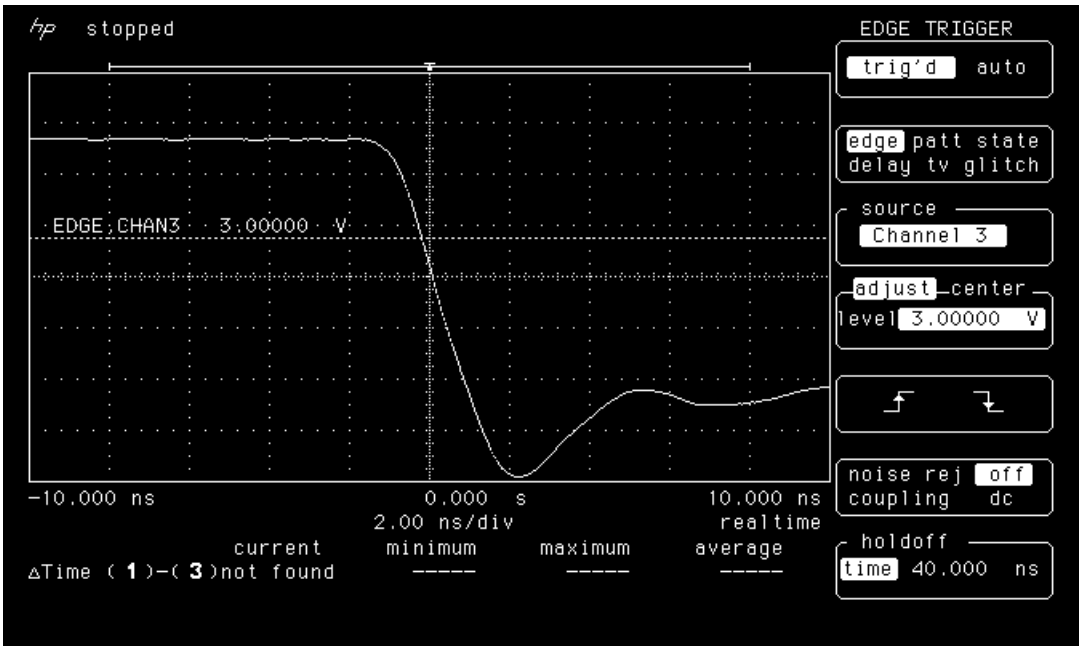


Figure 12c. Falling edge of LAN2001 post-anneal.

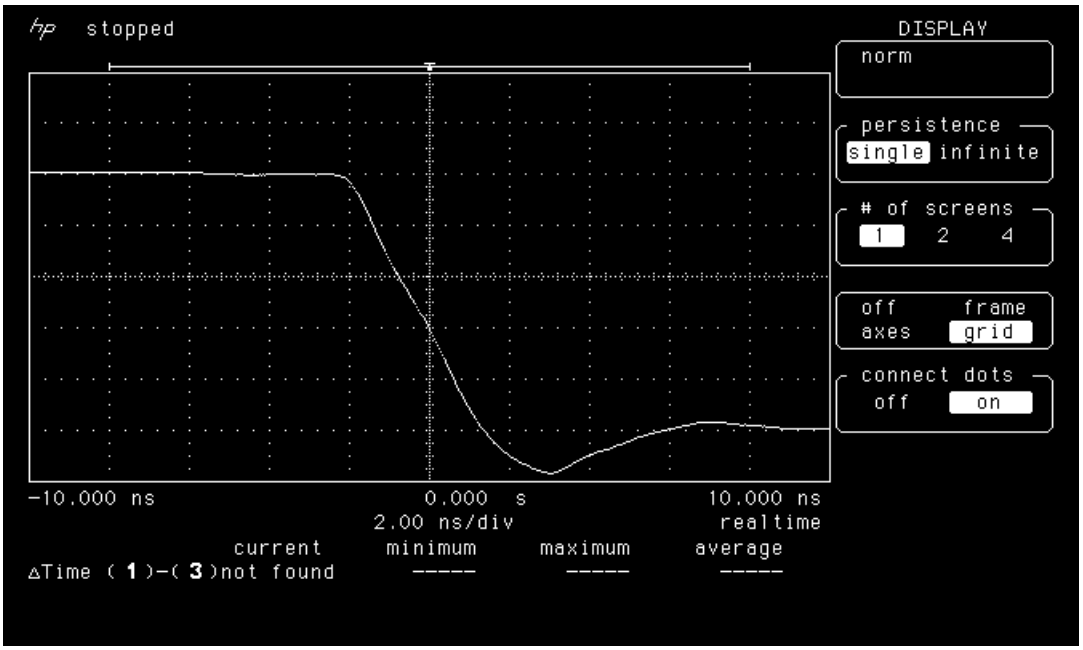


Figure 13a. Falling edge of LAN2002 pre-irradiation.

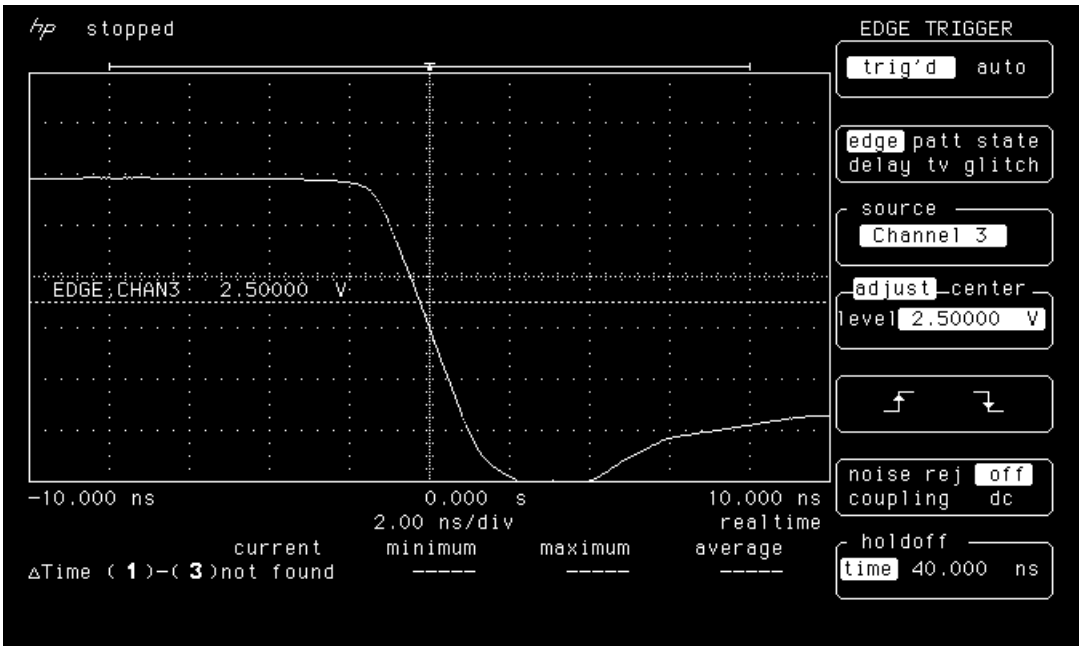


Figure 13b. Falling edge of LAN2002 post-irradiation

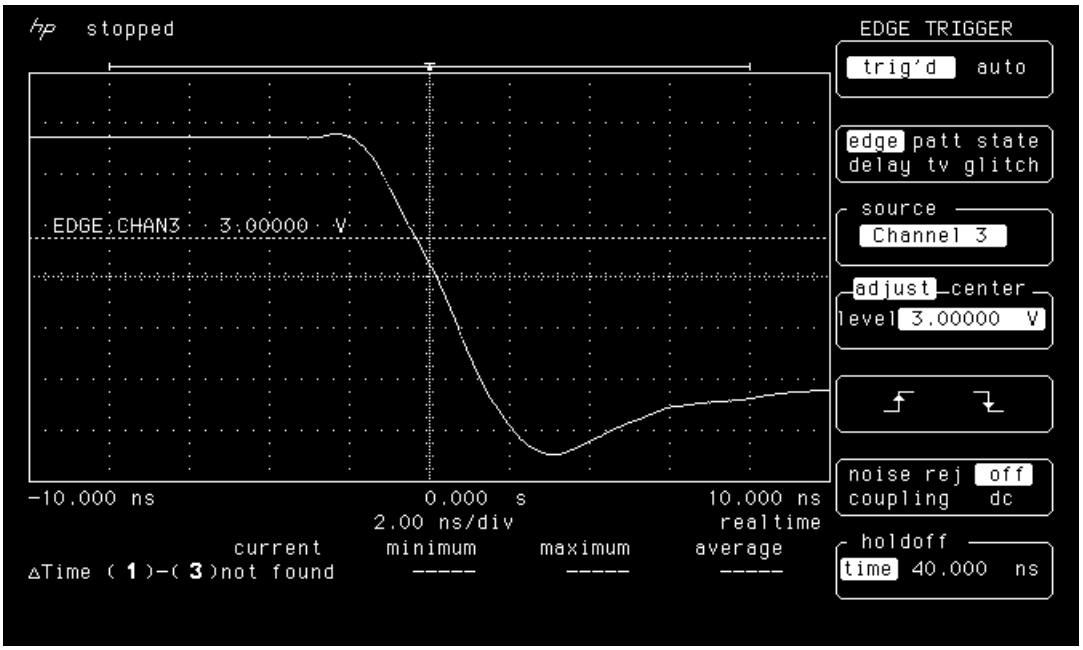


Figure 13c. Falling edge of LAN2002 post-anneal.

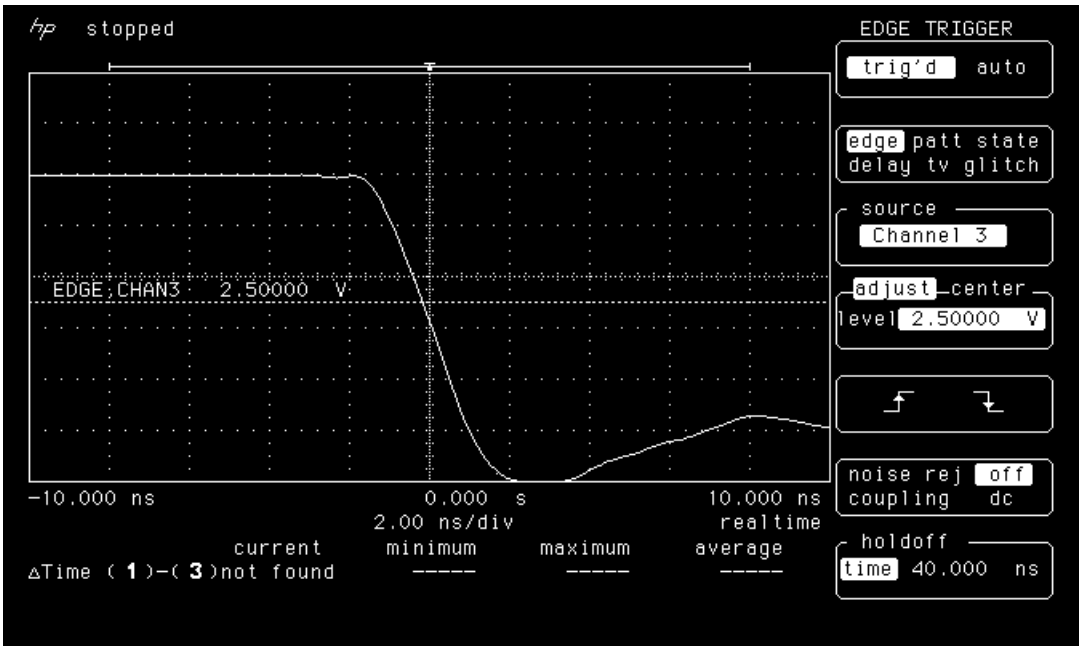


Figure 14a. Falling edge of LAN2003 pre-irradiation.

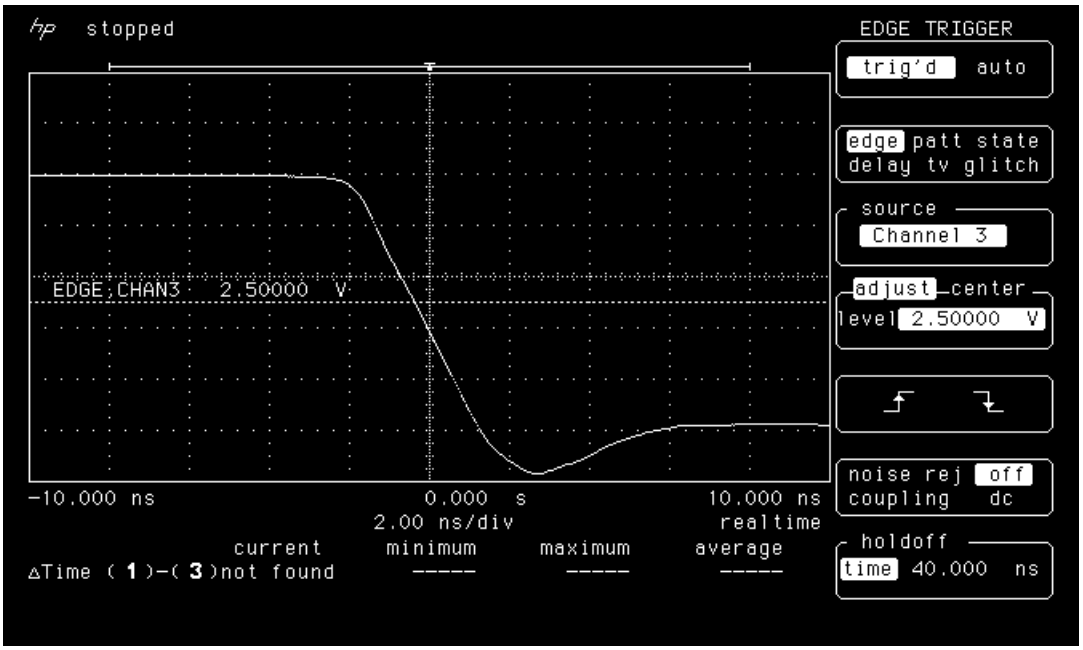


Figure 14b. Falling edge of LAN2003 post-irradiation.

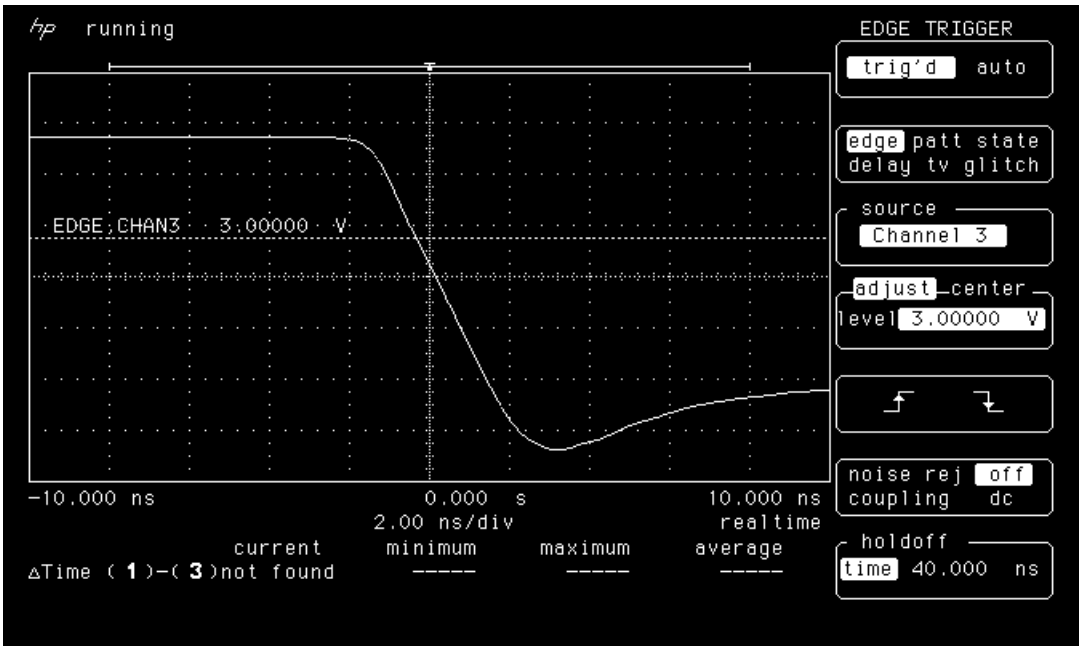


Figure 14c. Falling edge of LAN2003 post-anneal.

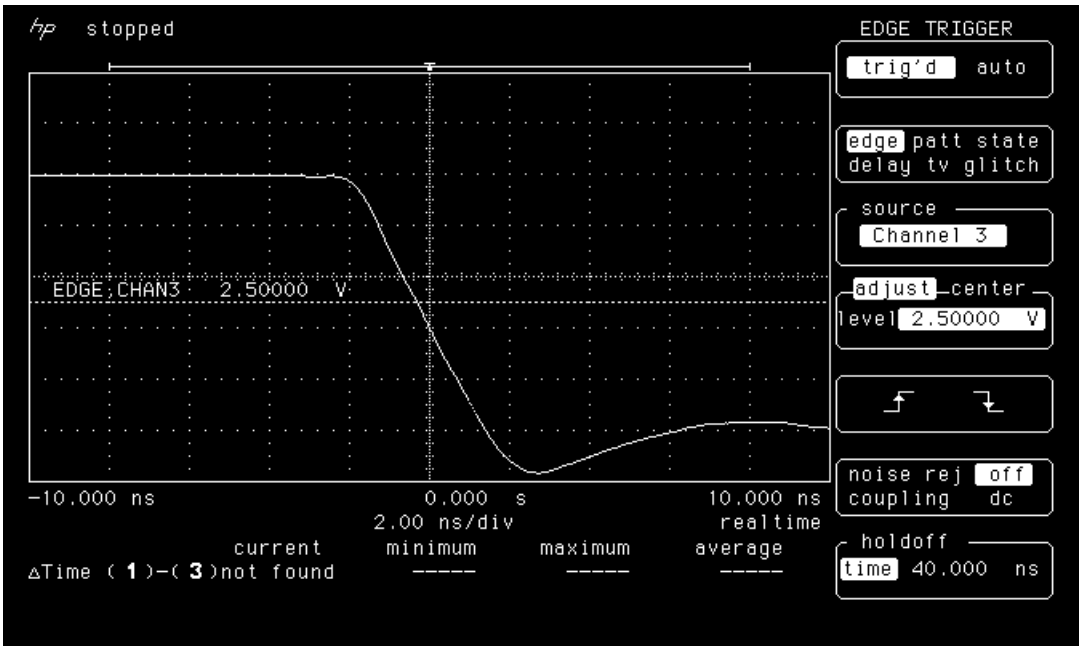


Figure 15a. Falling edge of LAN2004 pre-irradiation.

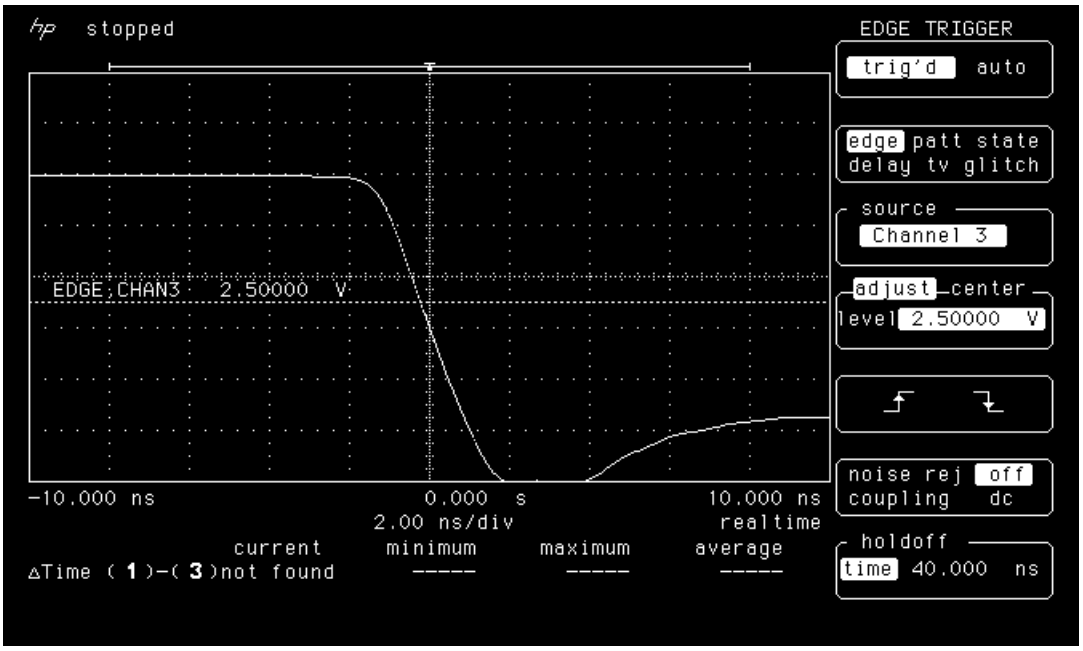


Figure 15b. Falling edge of LAN2003 post-irradiation.

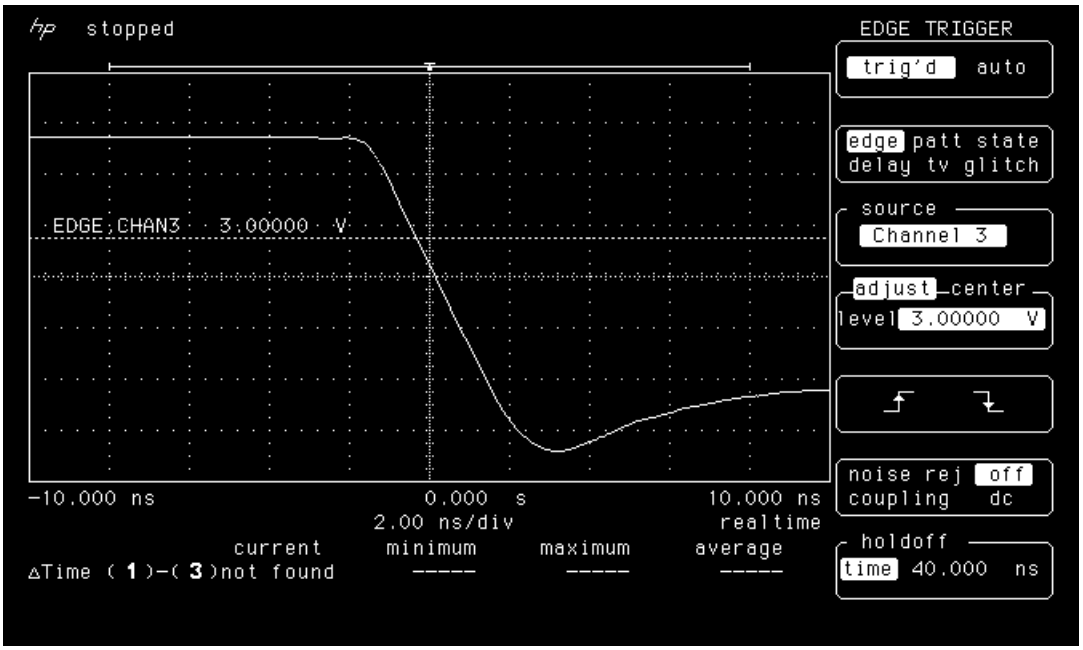


Figure 15c. Falling edge of LAN2003 post-anneal.

## 3.7 STARTUP TRANSIENT

In each measurement, the power supply ($V_{CC}$) rising time was set at 1.2ms. The board housing the DUT has minimum capacitance so that the transient current is all coming from the DUT. Figure 16-20 shows the oscilloscope picture of the startup transient of the DUTs. In each picture, there is a curve showing $V_{CC}$ ramping from GND to 5V, and another curve showing $I_{CC}$ which has a transient pulse at $V_{CC}$ close to 3V. The scale is 1V per division for $V_{CC}$ and 100mA per division for $I_{CC}$. The transient pulse of $I_{CC}$ is approximately 100mA peak and less than 100µs width. From these pictures, it can be concluded that the irradiation (within 20krad(Si) total dose) does not increase the transient pulse.

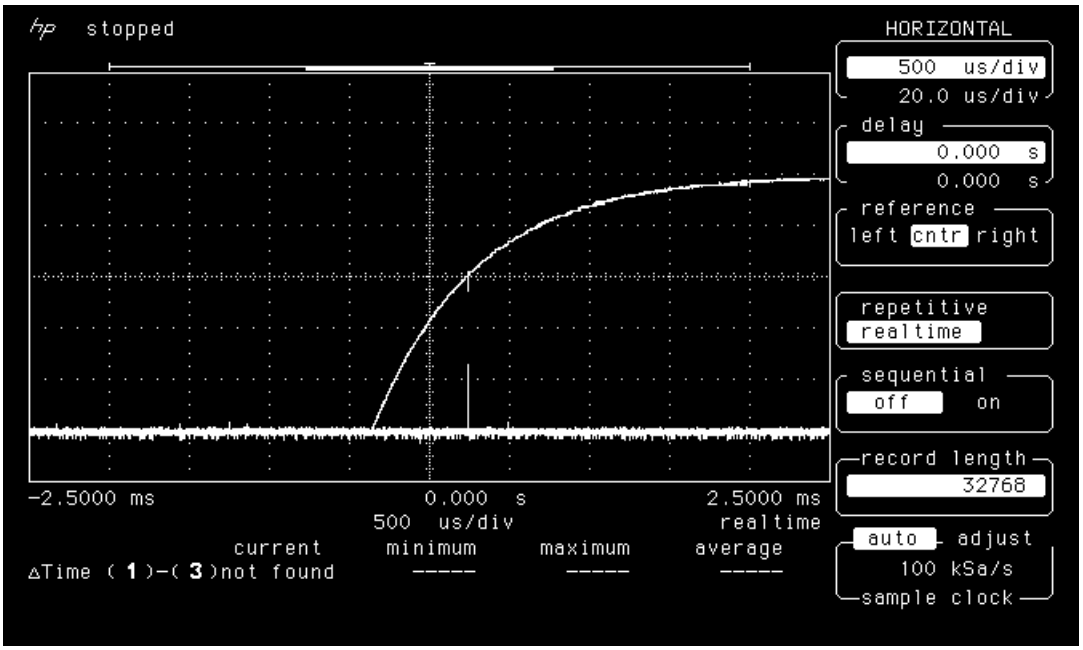


Figure 16a. Startup transient of LAN905 (control) measured with pre-irradiation DUTs.

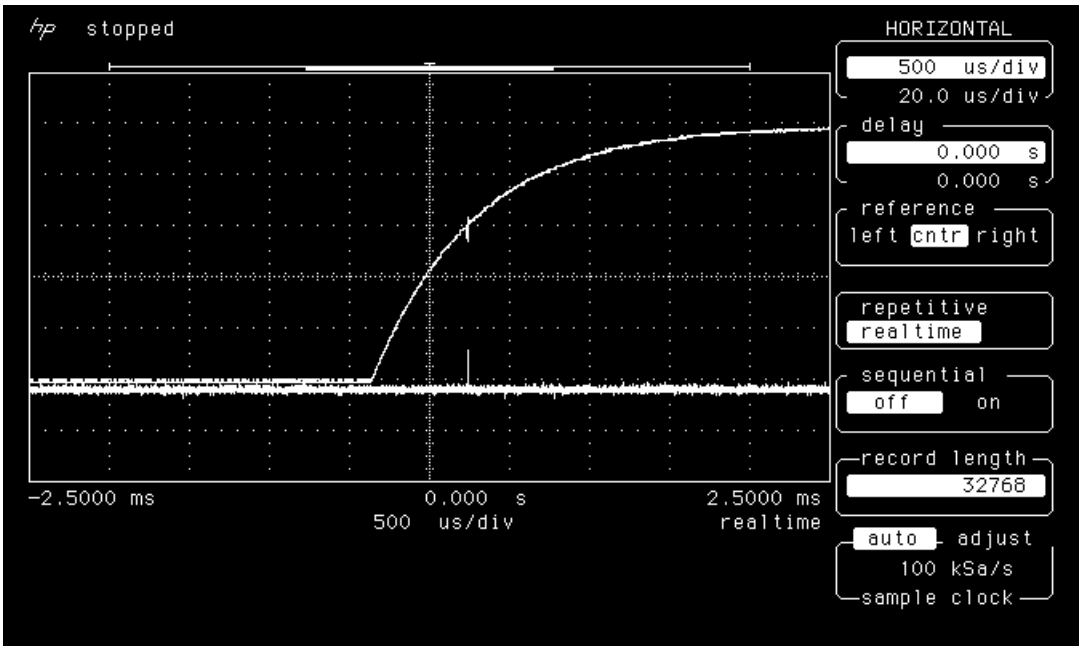


Figure 16b. Startup transient of LAN905 (control) measured with post-anneal DUTs

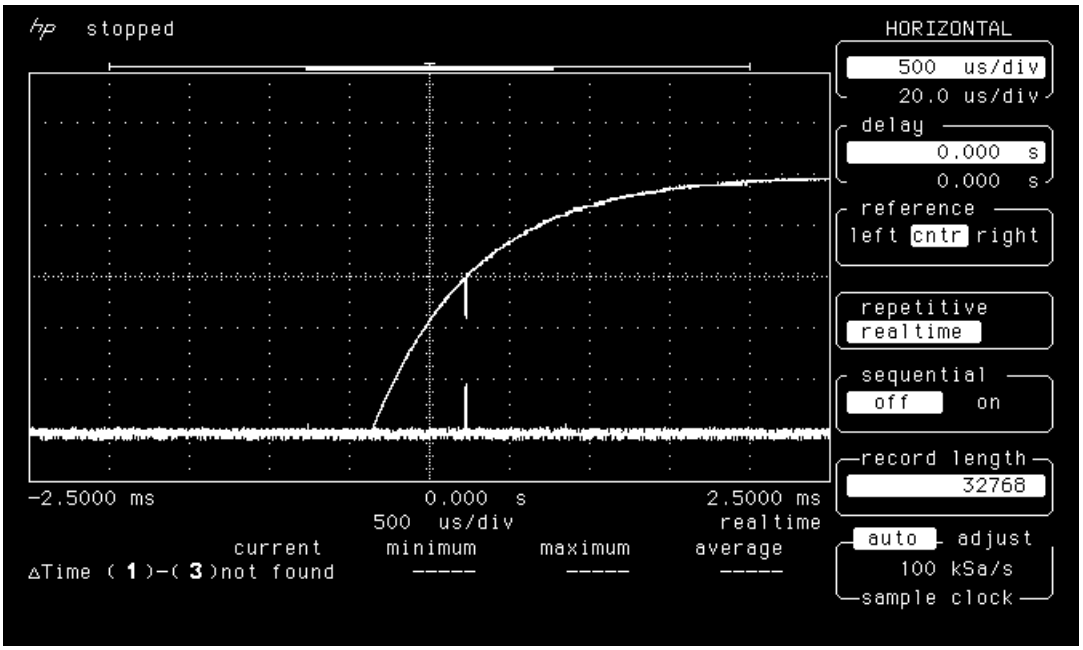


Figure 17a. Startup transient of LAN2001 pre-irradiation.

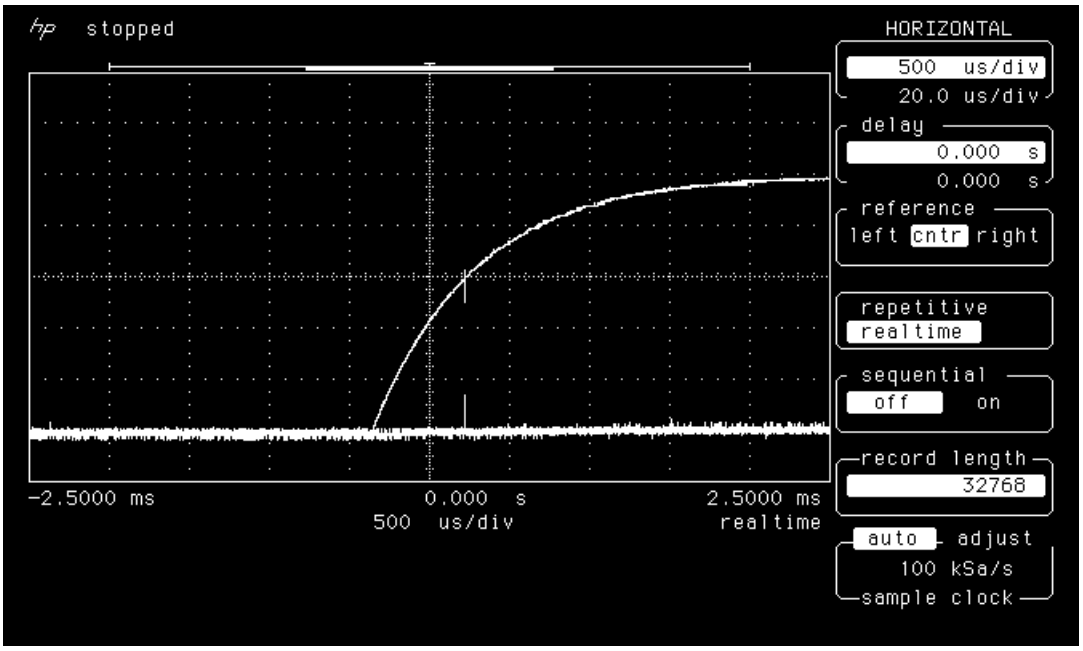


Figure 17b. Startup transient of LAN2001 post-irradiation.

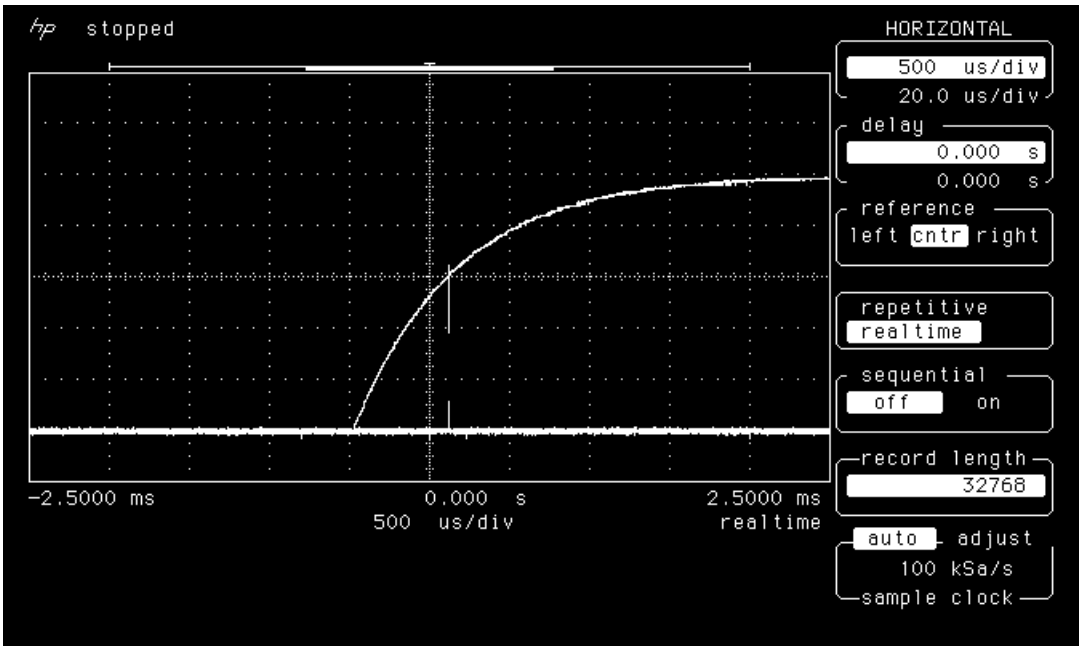


Figure 18a. Startup transient of LAN2002 pre-irradiation.

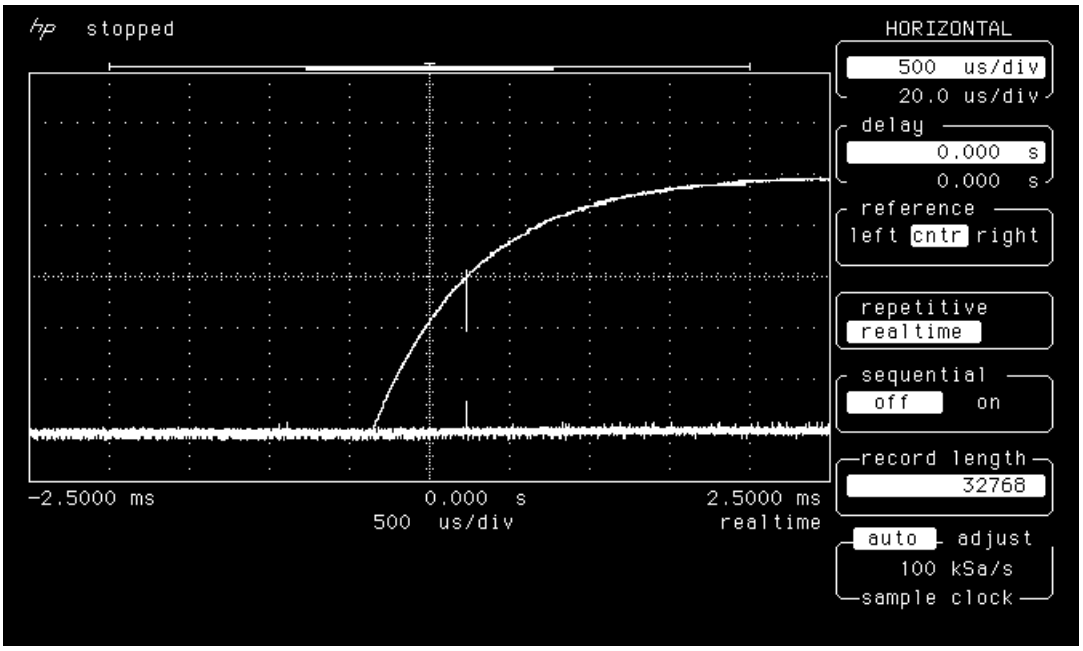


Figure 18b. Startup transient of LAN2002 post-irradiation

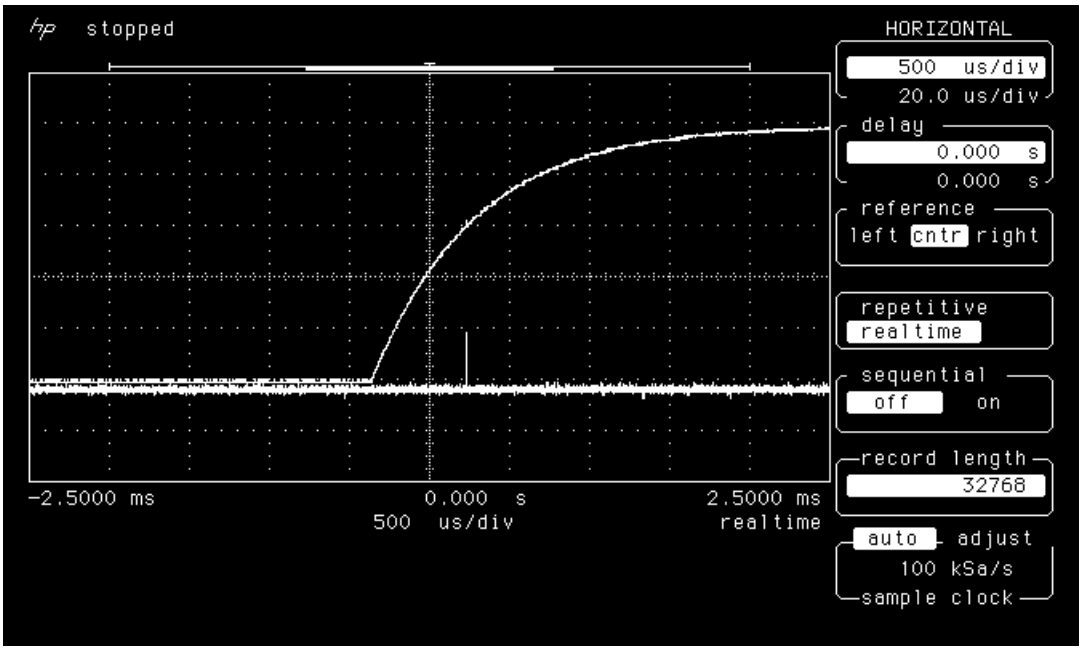


Figure 18c. Startup transient of LAN2002 post-anneal.

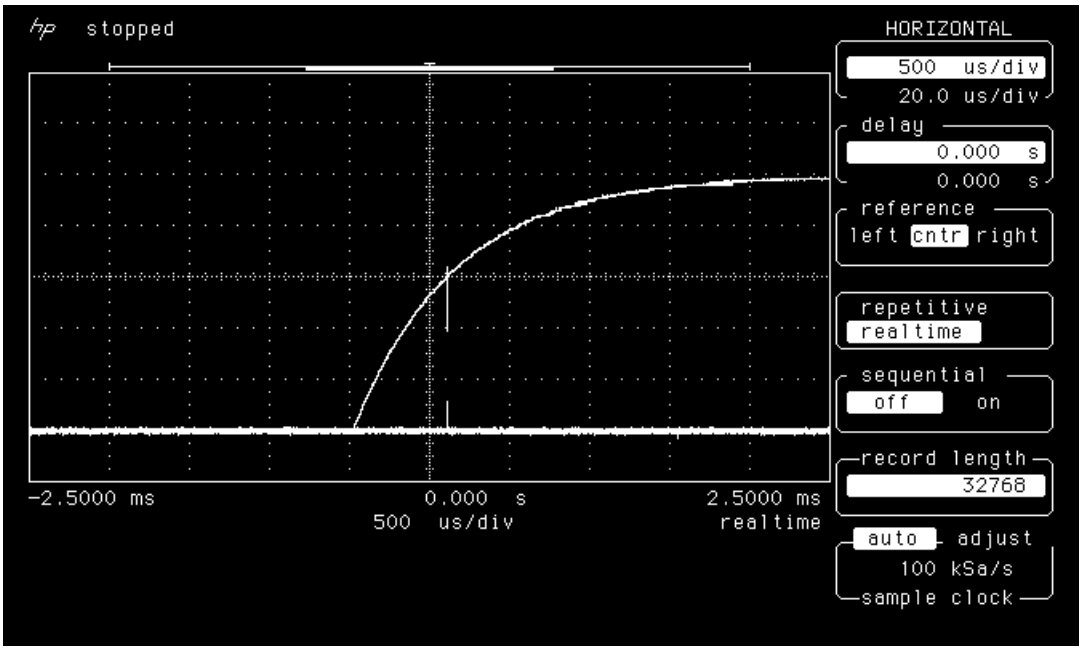


Figure 19a. Startup transient of LAN2003 pre-irradiation.

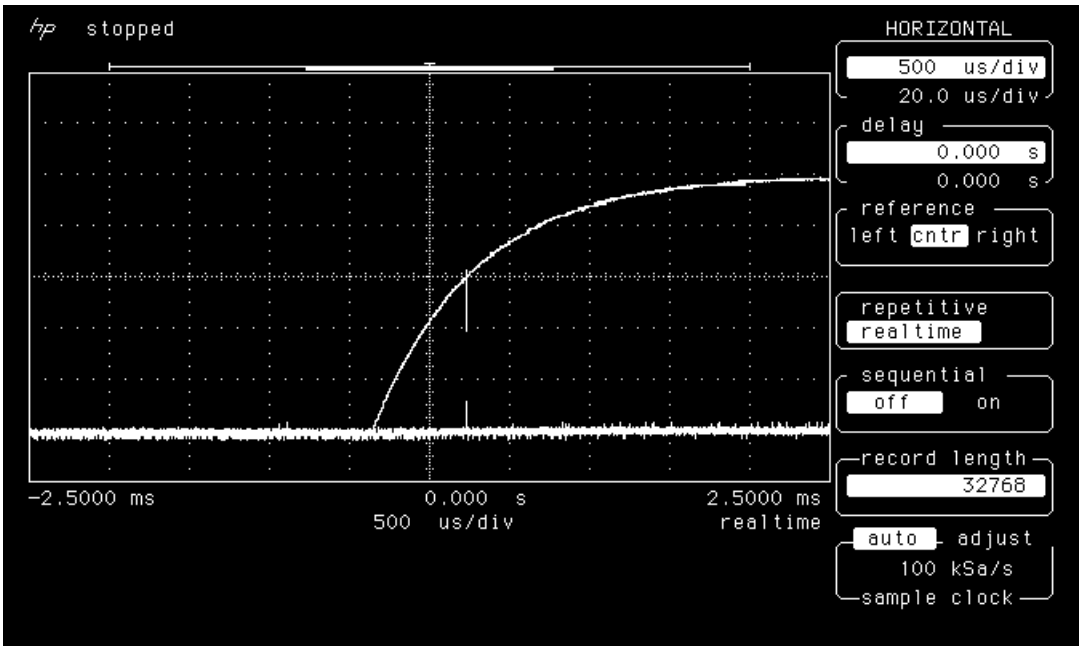


Figure 19b. Startup transient of LAN2003 post-irradiation.

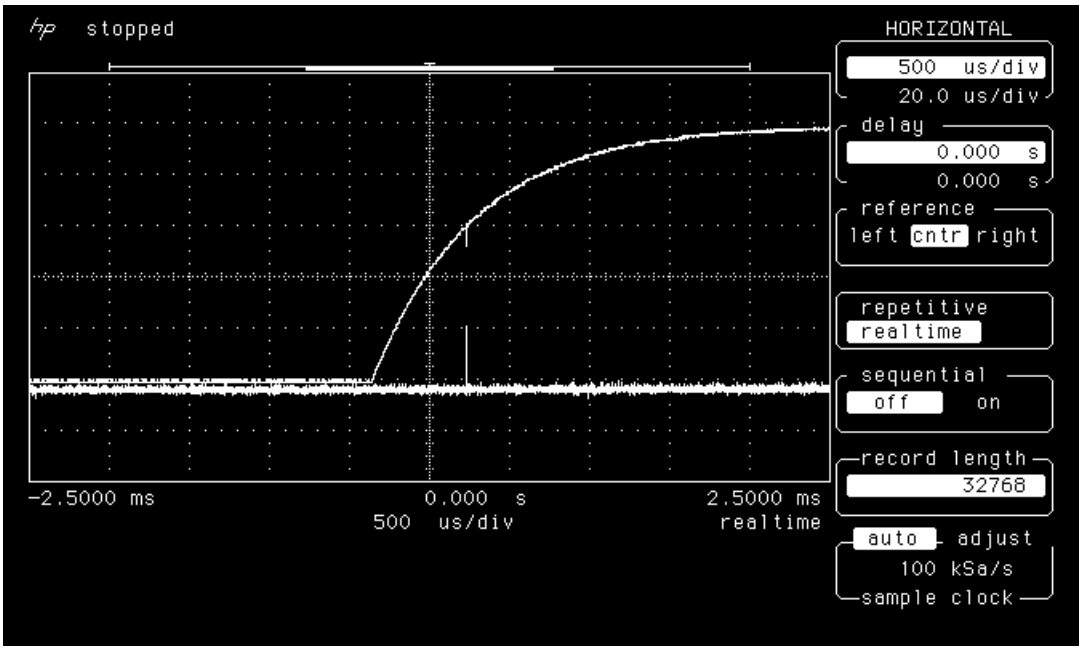


Figure 19c. Startup transient of LAN2003 post-anneal.

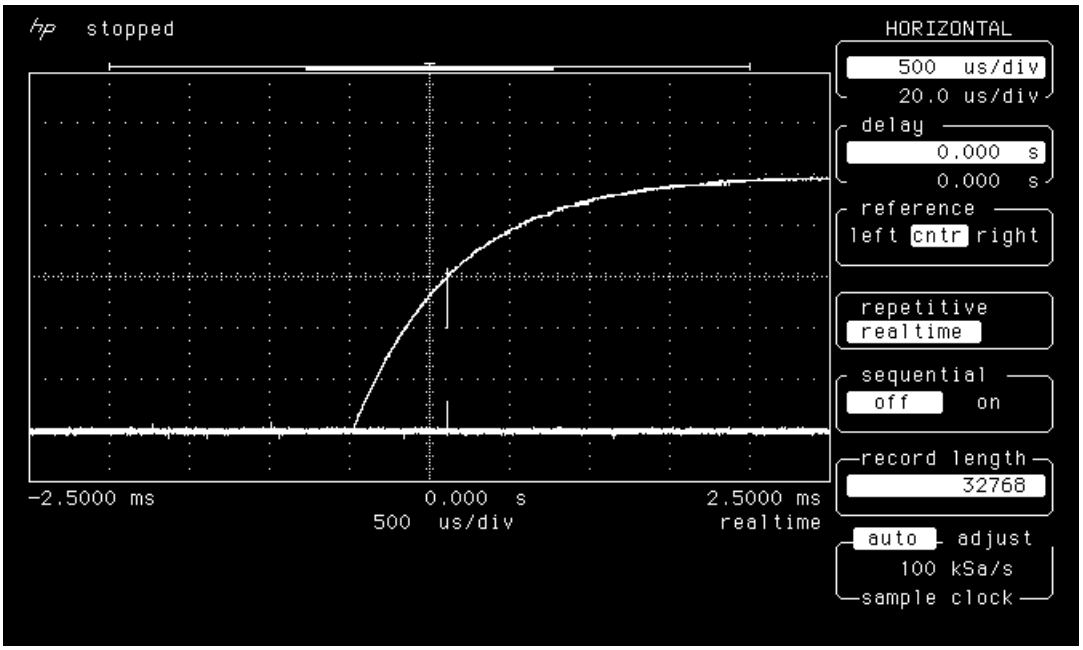


Figure 20a. Startup transient of LAN2004 pre-irradiation.

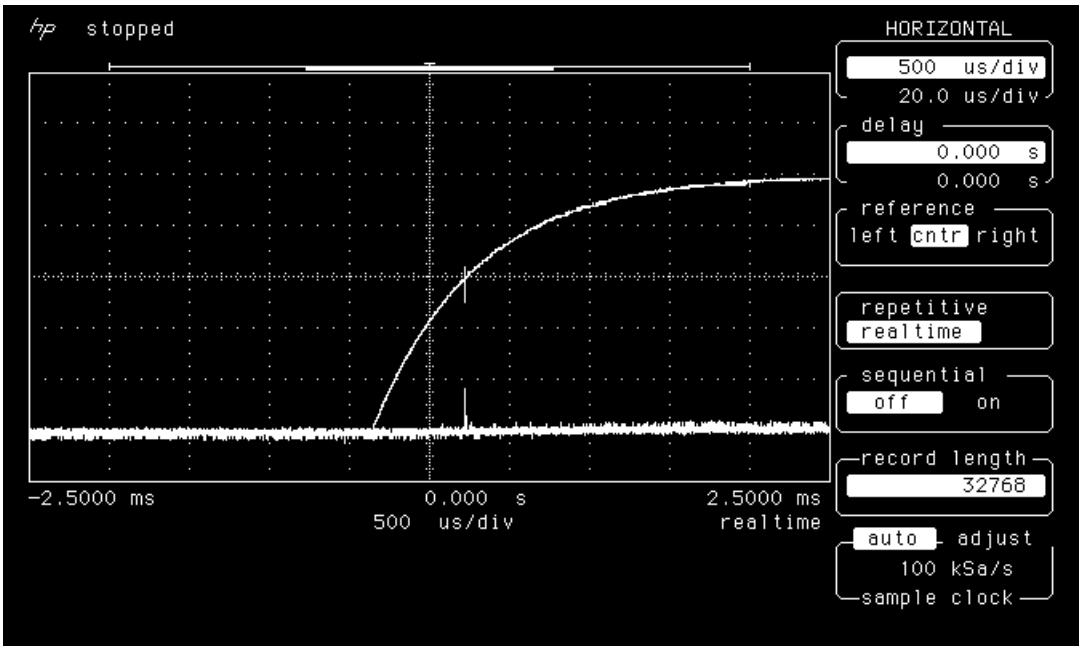


Figure 20b. Startup transient of LAN2004 post-irradiation.

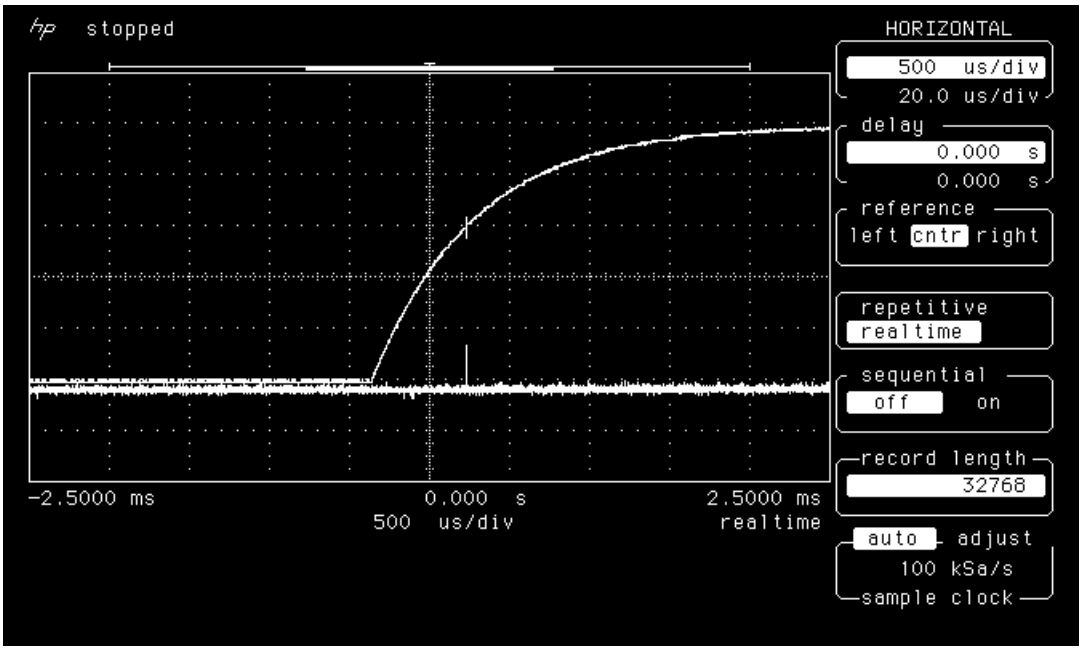


Figure 20c. Startup transient of LAN2004 post-anneal.